# PROBING THE INTERGALACTIC MEDIUM/GALAXY CONNECTION. V. ON THE ORIGIN OF Ly# AND O VI ABSORPTION AT z < 0.2

The Astrophysical Journal, 740:91 (22pp), 2011 October 20 doi:10.1088/0004-637X/740/2/91


# PROBING THE INTERGALACTIC MEDIUM/GALAXY CONNECTION. V. ON THE ORIGIN OF Lyα AND O VI ABSORPTION AT $z < 0.2$

J. Xavier Prochaska[1], B. Weiner[2], H.-W. Chen[3], J. Mulchaey[4], and K. Cooksey[5,6]
[1] Department of Astronomy and Astrophysics & UCO/Lick Observatory, University of California, 1156 High Street, Santa Cruz, CA 95064, USA; xavier@ucolick.org
[2] Steward Observatory, University of Arizona, 933 N. Cherry Ave., Tucson, AZ 85721, USA; bjw@as.arizona.edu
[3] Department of Astronomy, University of Chicago, 5640 S. Ellis Ave., Chicago, IL 60637, USA; hchen@oddjob.uchicago.edu
[4] Carnegie Observatories, 813 Santa Barbara St., Pasadena, CA 91101, USA; mulchaey@obs.carnegiescience.edu
[5] MIT Kavli Institute for Astrophysics & Space Research, 77 Massachusetts Avenue, 37-611, Cambridge, MA 02139, USA; kcooksey@space.mit.edu
*Received 2011 March 9; accepted 2011 July 21; published 2011 October 3*

## ABSTRACT

We analyze the association of galaxies with Lyα and O VI absorption, the most commonly detected transitions of the low-$z$ intergalactic medium (IGM), in the fields of 14 quasars with $z_{\rm em} = 0.06$–$0.57$. Confirming previous studies, we observe a high covering fraction for Lyα absorption to impact parameter $\rho = 300\ h_{72}^{-1}$ kpc: 33/37 of our $L > 0.01\ L^*$ galaxies show Lyα equivalent width $W^{\rm Ly\alpha} \geqslant 50$ mÅ. Galaxies of all luminosity $L > 0.01\ L^*$ and spectral type are surrounded by a diffuse and ionized circumgalactic medium (CGM), whose baryonic mass is estimated at $\sim 10^{10.5\pm0.3}\ M_\odot$ for a constant $N_{\rm H} = 10^{19}$ cm$^{-2}$. The virialized halos and extended CGM of present-day galaxies are responsible for most strong Lyα absorbers ($W^{\rm Ly\alpha} > 300$ mÅ) but cannot reproduce the majority of observed lines in the Lyα forest. We conclude that the majority of Lyα absorption with $W^{\rm Ly\alpha} = 30$–$300$ mÅ occurs in the cosmic web predicted by cosmological simulations and estimate a characteristic width for these filaments of $\approx 400\ h_{72}^{-1}$ kpc. Regarding O VI, we observe a near unity covering fraction to $\rho = 200\ h_{72}^{-1}$ kpc for $L > 0.1\ L^*$ galaxies and to $\rho = 300\ h_{72}^{-1}$ kpc for sub-$L^*$ ($0.1\ L^* < L < L^*$) galaxies. Similar to our Lyα results, stronger O VI systems ($W^{1031} > 70$ mÅ) arise in the virialized halos of $L > 0.1\ L^*$ galaxies. Unlike Lyα, the weaker O VI systems ($W^{1031} \approx 30$ mÅ) arise in the extended CGM of sub-$L^*$ galaxies. The majority of O VI gas observed in the low-$z$ IGM is associated with a diffuse medium surrounding individual galaxies with $L \approx 0.3\ L^*$ and rarely originates in the so-called warm-hot IGM (predicted by cosmological simulations.

*Key words:* galaxies: structure – intergalactic medium – large-scale structure of universe – quasars: absorption lines

*Online-only material:* color figures, machine-readable table

## 1. INTRODUCTION

Ultraviolet absorption-line spectroscopy remains the most efficient and sensitive means of studying the diffuse gas that permeates the universe. This gas, commonly referred to as the intergalactic medium (the IGM) or Lyα forest, is the dominant reservoir of baryons in the universe at all epochs (e.g., Prochaska & Tumlinson 2009). It provides fresh fuel for star formation and collects the radiation and metals produced by galaxies and active galactic nuclei (AGNs). Furthermore, the IGM is expected to trace the dark matter distribution of large-scale structure, offering unique constraints on our cosmological paradigm (e.g., Miralda-Escudé et al. 1996; Rauch 1998; McDonald et al. 2006; Viel et al. 2009).

Analysis of quasar spectra acquired with UV-sensitive spectrometers on the *Hubble Space Telescope* (*HST*) and *Far Ultraviolet Spectroscopic Explorer* (*FUSE*) have surveyed the redshift distribution, metal enrichment, ionization state, and temperature of the IGM in the $z < 1$ universe (e.g., Weymann et al. 1998; Davé et al. 1999; Prochaska et al. 2006; Thom & Chen 2008b; Tripp et al. 2008; Danforth & Shull 2008; Cooksey et al. 2010). These studies have demonstrated, similar to the high-$z$ IGM, that the gas collects in a set of relatively discrete "lines" in redshift, has a high ionization fraction, and is often enriched with heavy elements (e.g., C, O). The Lyα forest is significantly sparser at $z < 1$, however, because of the steady expansion of the universe. The cosmic abundance of heavy metals also appears to have evolved (e.g., Prochaska et al. 2004; Danforth & Shull 2008; Cooksey et al. 2010), although the scatter for individual regions is large.

Over the past decade, extra attention has been placed on the search for a warm-hot phase of the IGM ($T \gtrsim 10^5$ K) that is predicted by cosmological simulations to be a major baryonic reservoir in the low-$z$ universe (Cen & Ostriker 1999; Davé et al. 2001). In the UV, the search for this so-called warm-hot IGM (WHIM) includes surveys for the O VI doublet (e.g., Tripp et al. 2000, 2008; Thom & Chen 2008b), searches for thermally broadened Lyα lines (e.g., Lehner et al. 2007), and, most recently, surveys for Ne VIII absorption (Savage et al. 2005; Narayanan et al. 2009). Owing to its greater ease of detection, the O VI doublet has been the most frequently studied transition to date. Focused surveys have characterized its incidence as a function of equivalent width and column density (Tripp et al. 2008; Thom & Chen 2008b; Danforth & Shull 2008; Wakker & Savage 2009), and have permitted statistical comparison with predictions from cosmological simulations (e.g., Cen & Fang 2006; Oppenheimer & Davé 2009; Tepper-García et al. 2011; Smith et al. 2011; Oppenheimer et al. 2011).

Although UV spectral analysis provides robust constraints on the nature and distribution of diffuse gas, considerable debate remains over the origin and cosmological relevance of the observed absorption systems. For example, hot and diffuse gas is

[6] NSF Astronomy and Astrophysics Postdoctoral Fellow.

predicted (and observed) to exist in the outer halos of individual galaxies (Spitzer 1956; Bahcall & Spitzer 1969; Mo & Miralda-Escude 1996; Maller & Bullock 2004; Sembach et al. 2003), the intragroup medium (e.g., Mulchaey et al. 1996; Freeland et al. 2008), and also the filamentary structures of the IGM (e.g., Cen & Ostriker 1999). The incidence of O VI, therefore, is likely a sensitive function of how metals are dispersed on galactic and intergalactic scales and also the physical conditions within these various environments (e.g., Oppenheimer & Davé 2009). Not surprisingly, different research groups have drawn competing conclusions on whether the O VI absorbers primarily trace the low-density WHIM or a photoionized, cooler phase. Similarly, multiple scenarios may explain the incidence and properties of the Ly$\alpha$ "clouds" along single IGM sight lines. While ram-pressure stripping, tidal stripping, and galactic-scale winds are all believed to play a role in transporting gas from galaxies to the IGM, the timing and relative importance of each of these remain open issues. In short, there remain several fundamental questions on the origin and nature of the two most common transitions of the IGM.

Researchers have long recognized that additional insight into the IGM may be gained by surveying the fields surrounding absorption-line systems for galaxies and their large-scale structures. Early efforts focused on Ly$\alpha$ absorption and the relation of H I gas to galaxies and large-scale structures (Spinrad et al. 1993; Morris et al. 1993; Lanzetta et al. 1995). A key result was that sight lines with small impact parameters to galaxies ($\rho \lesssim 250\ h_{72}^{-1}$ kpc) had a high incidence of moderate to strong Ly$\alpha$ absorption (Lanzetta et al. 1995; Chen et al. 1998; Tripp et al. 1998; Chen et al. 2001b; Bowen et al. 2002; Morris & Jannuzi 2006). This indicates galaxies are surrounded by a diffuse, highly ionized medium that gives rise to significant Ly$\alpha$ absorption (see also Wakker & Savage 2009). These studies were followed by two-point cross-correlation analysis of galaxies to absorbers on $\approx$1 Mpc scales (Chen et al. 2005; Wilman et al. 2007; Chen & Mulchaey 2009) and have recently been extended to $z \sim 1$ (Shone et al. 2010). Their results reveal significant clustering between galaxies and strong Ly$\alpha$ systems (absorbers with H I column density, $N_{\rm H\,I} > 10^{15}\ {\rm cm}^{-2}$) that implies a causal connection. In contrast, these authors measure a very weak (or absent) clustering signal for low-$N_{\rm H\,I}$ absorption systems which implies the two phenomena trace different structures in the universe. While previous work has offered valuable insight into the nature of the Ly$\alpha$ forest, it is limited by sample variance both in terms of the number of absorbers, galaxies, and fields surveyed.

Several projects have now also considered the galaxy/absorber connection for the metal-enriched IGM, e.g., Mg II, C IV, and O VI selected systems. For the first, observers have commonly associated strong Mg II absorption with individual galaxies at impact parameters $\rho < 100$ kpc, by searching for galaxies at the redshifts of known Mg II systems (e.g., Bergeron 1986; Bergeron & Boisse 1991). Indeed, galaxies at low $z$ show modest to high covering fractions of cool gas ($T \sim 10^4$ K) traced by Mg II absorption (Chen & Tinker 2008; Barton & Cooke 2009; Chen et al. 2010) with the covering fraction apparently dependent on galaxy type (Gauthier et al. 2010; Bowen & Chelouche 2011). This has led to the association of metal-enriched, cool IGM gas with the "halos" of individual galaxies. Galaxies also exhibit a high covering fraction to C IV absorption for impact parameters $\rho \lesssim 200$ kpc (Chen et al. 2001a). Although the origin of this highly ionized gas is not well established, these results likely require a multi-phase medium in the virialized halos of modern galaxies (Mo & Miralda-Escude 1996; Maller & Bullock 2004).

The O VI doublet has long been recognized to trace a highly ionized, warm/hot phase of the Galaxy. The original detections associated O VI gas with supernova remnants in the disk (Jenkins & Meloy 1974; York 1974). A statistical analysis of O VI absorption toward extragalactic sources with *FUSE* suggests a thick layer of highly ionized gas with a scale height of $\approx$3 kpc (Savage et al. 2000; Bowen et al. 2008). Lastly, studies of highly ionized gas toward extragalactic sources reveal a high covering fraction from an inferred halo of collisionally ionized gas at $T \approx 10^5$ K (Savage & de Boer 1979; Savage et al. 2003; Sembach et al. 2006). Similar halos of O VI-bearing gas have been inferred for external galaxies through O VI emission maps (Bregman et al. 2005). It is evident that some fraction of the O VI observed in the IGM must arise from galactic halos.

Connecting O VI gas of the IGM to galaxies and the structures they reside within has been the focus of several recent studies. In Prochaska et al. (2006), we examined the field surrounding the multiple O VI systems identified along the sight line to PKS0405–123. While the strong absorption at $z = 0.167$ was notable for its association with two galaxies at small impact parameter ($\rho \sim 100$ kpc), additional O VI systems showed no obvious galactic counterparts and/or galaxies only at large impact parameter. A similar diversity of galactic environment has been observed for other sight lines (Shull et al. 2003; Sembach et al. 2004; Tumlinson et al. 2005; Tripp et al. 2006a; Cooksey et al. 2008; Chen & Mulchaey 2009). Stocke et al. (2006) performed the first multi-sight line analysis on the galaxy/absorber connection for O VI. For the nine O VI systems in their fields complete to 0.1 $L^*$ galaxies, they estimated a median distance to an $L \geqslant 0.1\,L^*$ galaxy of $\approx$180 $h_{70}^{-1}$ kpc. Furthermore, they identified an $L^*$ galaxy within 800 $h_{70}^{-1}$ kpc for essentially each of the 23 O VI absorbers in their survey. They inferred, based on these results, that O VI gas does not occur in galaxy voids. They further hypothesized that galaxies with $L \leqslant 0.1\,L^*$ galaxies may be most responsible for O VI absorption. Similar results were found by Wakker & Savage (2009) for a small sample of $z \approx 0$ galaxies.

Recently, we published the results of a galaxy survey performed with the WFCCD spectrometer on the 100″ Dupont telescope at Las Campanas Observatory (LCO) in the fields surrounding 20 UV-bright quasars at $z < 1$ (Prochaska et al. 2011). The principal motivation for this survey was to assess the galaxy/absorber connection for O VI gas at $z \leqslant 0.2$. In this paper, we present the first scientific results from our complete survey. Previous papers studied the galaxy/IGM connection in a few, individual fields (Prochaska et al. 2004; Cooksey et al. 2008; Chen et al. 2005; Lehner et al. 2009). A future paper will study the cross-correlation function between galaxies and Ly$\alpha$/O VI absorbers.

This paper is organized as follows. In Section 2, we summarize the data sets that comprise the galaxy surveys (Prochaska et al. 2011) and the characterization of the IGM along the sight lines. The primary results of our analysis of galaxy/absorber association for Ly$\alpha$ and O VI are given in Section 3. We discuss the implications for the low-$z$ IGM of these results and their context with respect to previous work in Section 4 and we conclude with a summary in Section 5. Unless otherwise specified, we adopt a $\Omega_\Lambda = 0.74$, $\Omega_m = 0.26$, $H_0 = 72\,{\rm km\,s^{-1}\,Mpc^{-1}}$ cosmology (Dunkley et al. 2009). Furthermore, all distances are quoted in proper units unless otherwise noted.

**Table 1**
LCO/WFCCD Fields Analyzed

| Quasar | R.A. (J2000) | Decl. (J2000) | $z_{em}$ | *HST* UV Spectroscopic Data Sets | *FUSE*[a] | Ly$\alpha$ Ref. | O VI Ref. | $\mathcal{N}_{spec}$[b] |
|---|---|---|---|---|---|---|---|---|
| Q0026+1259 | 00:29:13.8 | +13:16:04 | 0.142 | GHRS/(G270M) | 20 | | 9 | 60 |
| TonS 180 | 00:57:20.0 | −22:22:56 | 0.062 | STIS/(G140M,G230MB) | 132 | 5 | 4 | 7 |
| PKS0312−77 | 03:11:55.2 | −76:51:51 | 0.223 | STIS/(E140M) | | 3 | 1,3 | 56 |
| PKS0405−123 | 04:07:48.4 | −12:11:37 | 0.573 | STIS/(E140M,G230M); GHRS/(G160M,G200M) | 71 | 3,4,9 | 1,3,4,9 | 565 |
| PG1004+130 | 10:07:26.1 | +12:48:56 | 0.240 | STIS/(G140M) | 85 | 9 | 9 | 61 |
| HE1029−140 | 10:31:54.3 | −14:16:51 | 0.086 | STIS/(G140M) | | 5 | | 8 |
| PG1116+215 | 11:19:08.70 | +21:19:18 | 0.176 | STIS/(G140M,E140M,E230M); GHRS/(G140L) | 76 | 1,3,4,5,9 | 1,2,3,4 | 74 |
| PG1211+143 | 12:14:17.7 | +14:03:13 | 0.081 | STIS/(G140M,E140M); GHRS/(G140L,G270M) | 52 | 3,4,5 | 3,4 | 25 |
| PG1216+069 | 12:19:20.9 | +06:38:38 | 0.331 | STIS/(E140M); GHRS/(G140L) | 13 | 1,3,6,9 | 1,2,3,9 | 101 |
| 3C273 | 12:29:6.70 | +02:03:9.0 | 0.158 | STIS/(E140M); GHRS/(FG130,FG190,FG270,G160M) | 42 | 1,3,4,9 | 1,2,3,4 | 32 |
| PKS1302−102 | 13:05:33.0 | −10:33:19 | 0.286 | STIS/(E140M) | 140 | 3,4,9 | 1,3,4,9 | 63 |
| MRK1383 | 14:29:06.4 | +01:17:06.0 | 0.086 | STIS/(E140M,G140M) | 64 | 3,4,5 | 4,9 | 5 |
| FJ2155−0922 | 21:55:01.5 | −09:22:25.0 | 0.192 | STIS/(E140M,G230MB) | 46 | 1,3,4,9 | 1,2,3,4,9 | 105 |
| PKS2155−304 | 21:58:51.8 | −30:13:30.0 | 0.116 | STIS/(E140M); GHRS/(G160M,ECH-B,G140L) | 123 | 3,4,9 | 3,4 | 43 |

**Notes.**
[a] Total integration time in ks.
[b] Number of spectroscopically determined galaxy redshifts for objects with $0.005 < z < z_{em}$.
**References.** (1) Tripp et al. 2008; (2) Thom & Chen 2008b; (3) Danforth & Shull 2008; (4) Danforth et al. 2006; (5) Penton et al. 2004; (6) Chen & Mulchaey 2009; (9) this paper.

## 2. DATA SETS

### 2.1. The LOC/WFCCD Galaxy Survey

We have recently published a survey of galaxies in the fields of 20 quasars with bright UV fluxes (Paper IV), the majority of which have UV spectral data sets that yield precise measurements of Ly$\alpha$ and/or O VI absorption (Table 1). The galaxy survey was performed with the WFCCD spectrometer on the 100″ Dupont telescope and was designed to achieve a high level of completeness to $R \leqslant 19.5$ mag galaxies in an $\approx 20' \times 20'$ field centered on each quasar. These survey parameters were chosen to recover dwarf galaxies ($L < 0.1\,L^*$) to at least $z = 0.1$ and to span an $\approx$1 Mpc impact parameter at $z \approx 0.1$. With this experimental design, we aimed to study the galaxies and their structures (e.g., groups) associated with IGM absorption. In several analyses, we also include the galaxy survey in the field of PKS0405–123 published by Williger et al. (2006).

The fields were selected on the basis of the quasar redshift (higher $z$ was preferred) and UV flux, with some preference given to fields with existing UV spectroscopic data sets. None of the fields were chosen because of the presence of known absorption systems, although an O VI-bearing Lyman limit system at $z = 0.167$ toward PKS0405–123 had been analyzed by our group previously (Chen & Prochaska 2000). As such, the galaxies discovered by our survey provide an unbiased sample that can then be searched for associated hydrogen and metal-line absorption.

This LCO/WFCCD galaxy survey provides the galaxy sample for the following analysis; we consider the results from complementary surveys in the discussion that follows (Section 4). Altogether, the LCO/WFCCD galaxy survey comprises 1198 galaxies with $0.005 < z < (z_{em} - 0.01)$ with a median redshift of 0.18. The distribution of their luminosities peaks near $\approx 0.3\,L^*$ and extends to $0.01\,L^*$ and $\approx 5\,L^*$.

### 2.2. IGM Surveys for Ly$\alpha$ and O VI Absorption

In the following IGM/galaxy analysis, we leverage published surveys for Ly$\alpha$ and O VI absorption in the quasar spectra of our fields. This corresponds to 13 sight lines with UV spectra from the *HST*/GHRS, *HST*/STIS, and/or *FUSE* instruments (Table 1). We restrict our analysis to surveys based on high spectral resolution data which generally provide equivalent-width sensitivity $\sigma(W)$ to a few tens of mÅ. Although the published surveys occasionally disagree on the identification of a particular line or on the confidence of its detection, we have not attempted to reconcile these arguments. Instead, we adopt all published detections as bona fide systems. In either case, our results do not depend sensitively on the positive existence of low-confidence lines. We have also restricted the number of references to key survey papers to have the samples drawn from as few sets of selection criteria as possible. When multiple groups have reported measurements for the same system, we have adopted the values from publications in this order: [Ly$\alpha$]—Tripp et al. (2008); Danforth & Shull (2008); Chen & Mulchaey (2009); Danforth et al. (2006); Penton et al. (2004); [O VI]—Tripp et al. (2008); Thom & Chen (2008b); Danforth & Shull (2008); Danforth et al. (2006). Because we rely primarily on published surveys (see below), the IGM results were derived independently of our galaxy survey.

For galaxies within several hundred kpc (up to 1 Mpc for Ly$\alpha$) of these sight lines, we have also done a focused search for associated Ly$\alpha$ and O VI absorption at their redshifts. Specifically, if there were no published measurement near the redshift of the galaxy yet spectra exist we reanalyzed the data ourselves. Furthermore, sufficient quality UV spectra exist for Ly$\alpha$ and/or O VI analysis in one of the LCO/WFCCD survey fields yet none has been published (Q0026+1259). We have also done a focused analysis in this sight line according to galaxies discovered in the LCO/WFCCD survey. To perform this new IGM analysis, we used spectra reduced by the instrument pipelines as described in Cooksey et al. (2008). We normalized the quasar continuum with automated algorithms and measured equivalent widths (and errors) with simple boxcar summation. If no absorption was present within $\pm 400\,\mathrm{km\,s^{-1}}$ of the galaxy redshift, we report a $3\sigma$ upper limit to the equivalent width and column density (assuming the linear curve-of-growth approximation). For positive detections, we measured column densities with the apparent optical depth method (Savage & Sembach 1991). In a few cases, the predicted wavelength of an Ly$\alpha$ or O VI line coincides

**Table 2**
New Targeted Search for Ly$\alpha$ and O VI Absorption associated with Galaxies

| Quasar | R.A. (J2000) | Decl. (J2000) | $z_{gal}$ | $W^{Ly\alpha}$ (Å) | $N_{H\,I}$ | $W^{O\,VI}$ (mÅ) | $N_{O\,VI}$ | UV Spectra |
|---|---|---|---|---|---|---|---|---|
| Q0026+1259 | 00:29:13.8 | +13:16:04 | 0.03290 | ... | ... | <120 | <14.0 | *FUSE* |
| | | | 0.03930 | ... | ... | <120 | <14.0 | *FUSE* |
| | | | 0.09610 | ... | ... | <100 | <14.0 | *FUSE* |
| | | | 0.11250 | ... | ... | <100 | <14.0 | *FUSE* |
| PKS0405−123 | 04:07:48.4 | −12:11:37 | 0.04320 | <0.03 | <12.7 | ... | ... | STIS/E140M |
| | | | 0.07910 | <0.03 | <12.7 | < 40 | <13.5 | *FUSE*, STIS/E140M |
| | | | 0.08000 | <0.03 | <12.7 | < 40 | <13.5 | *FUSE*, STIS/E140M |
| | | | 0.15220 | ... | ... | < 50 | <13.6 | STIS/E140M |
| | | | 0.20300 | <0.05 | <13.0 | < 30 | <13.4 | STIS/E140M |
| | | | 0.20890 | <0.03 | <12.7 | ... | ... | STIS/E140M |
| | | | 0.24840 | <0.05 | <12.9 | < 30 | <13.4 | STIS/E140M |
| | | | 0.28000 | <0.03 | <12.8 | ... | ... | STIS/E140M |
| | | | 0.29510 | <0.09 | <13.2 | < 30 | <13.4 | STIS/E140M |
| | | | 0.29760 | ... | ... | < 50 | <13.6 | STIS/E140M |
| | | | 0.30990 | <0.04 | <12.9 | < 40 | <13.5 | STIS/E140M |
| | | | 0.32030 | <0.05 | <13.0 | < 30 | <13.4 | STIS/E140M |
| | | | 0.32520 | ... | ... | < 50 | <13.6 | STIS/E140M |
| | | | 0.34150 | <0.15 | <13.5 | ... | ... | STIS/E140M |
| | | | 0.36810 | <0.05 | <13.0 | ... | ... | STIS/E140M |
| | | | 0.37850 | <0.06 | <13.0 | ... | ... | STIS/E140M |
| PG1004+130 | 10:07:26.1 | +12:48:56 | 0.00920 | 0.26 ± 0.03 | 13.9 ± 0.15 | <50 | <13.6 | *FUSE*, STIS/G140M |
| | | | 0.03008 | ... | ... | <200 | <14.5 | *FUSE* |
| | | | 0.07040 | ... | ... | <100 | <13.9 | *FUSE* |
| | | | 0.16740 | ... | ... | < 80 | <13.8 | STIS/G140M |
| | | | 0.19310 | ... | ... | <80 | <13.8 | STIS/G140M |
| PG1216+069 | 12:19:20.9 | +06:38:38 | 0.00630 | 2.32 ± 0.06 | 19.3 ± 0.05 | <200 | <14.2 | *FUSE*, STIS/E140M |
| | | | 0.00810 | <0.06 | <13.1 | <200 | <14.2 | *FUSE*, STIS/E140M |
| | | | 0.01262 | 0.35 ± 0.03 | >14.1 | <200 | <14.2 | *FUSE*, STIS/E140M |
| | | | 0.08150 | ... | ... | <120 | <14.0 | *FUSE* |
| | | | 0.11840 | <0.03 | <12.7 | <130 | <14.1 | *FUSE*, STIS/E140M |
| | | | 0.11910 | <0.03 | <12.7 | <130 | <14.1 | *FUSE*, STIS/E140M |
| | | | 0.13540 | ... | ... | <130 | <14.1 | *FUSE* |
| | | | 0.18100 | ... | ... | < 80 | <13.8 | STIS/E140M |
| | | | 0.19170 | <0.05 | <12.9 | < 40 | <13.5 | STIS/E140M |
| | | | 0.24640 | <0.05 | <12.9 | < 40 | <13.5 | STIS/E140M |
| | | | 0.27950 | <0.05 | <12.9 | < 60 | <13.6 | STIS/E140M |
| | | | 0.28000 | <0.05 | <12.9 | < 60 | <13.6 | STIS/E140M |
| PKS1302−102 | 13:05:33.0 | −10:33:19 | 0.02520 | <0.10 | <13.3 | < 40 | <13.5 | *FUSE*, STIS/E140M |
| | | | 0.03650 | <0.25 | <15.0 | ... | ... | STIS/E140M |
| | | | 0.05690 | <0.35 | <15.0 | < 40 | <13.5 | *FUSE*, STIS/E140M |
| | | | 0.07120 | <0.50 | <16.0 | < 40 | <13.5 | *FUSE*, STIS/E140M |
| | | | 0.07180 | <0.50 | <16.0 | < 40 | <13.5 | *FUSE*, STIS/E140M |
| | | | 0.10620 | <0.05 | <12.9 | ... | ... | STIS/E140M |
| | | | 0.13930 | <0.04 | <12.8 | ... | ... | STIS/E140M |
| | | | 0.14290 | <0.04 | <12.9 | < 40 | <13.5 | *FUSE*, STIS/E140M |
| MRK1383 | 14:29:06.4 | +01:17:06.0 | 0.02990 | ... | ... | < 40 | <13.5 | *FUSE* |

**Note.** The $N_{H\,I}$ value for the $z = 0.0063$ absorber toward PG1216+069 is taken from Tripp et al. (2005).

with Galactic ISM absorption or a coincident transition from another absorption system. In these events, we adopt the equivalent width of the coincident line as an upper limit to the equivalent width.

The measurements for our IGM analysis are summarized in Table 2. Altogether, we have useful constraints on Ly$\alpha$ and/or O VI absorption for 14 of our WFCCD survey fields.

## 3. RESULTS

We take two complementary approaches to the analysis: (1) we examine all galaxies that lie close to the sight lines for associated Ly$\alpha$ and O VI absorption and (2) we search the fields for galaxies associated with detected Ly$\alpha$ and O VI absorbers. Each of these techniques has specific strengths and weaknesses for interpreting the IGM/galaxy connection, as described below. Together, however, they provide powerful insight into the nature of the IGM and its interplay with galaxies at $z \sim 0$.

In the following, we establish the velocity criterion for associating a galaxy with IGM absorption (or vice versa) to be a velocity difference $|\delta v| < 400\,\mathrm{km\,s^{-1}}$. This value was chosen to be large enough to account for error in the galaxy redshifts (Prochaska et al. 2011) and to allow for velocities between the galaxy and gas that are characteristic of galactic dynamics. We emphasize that over 80% of the purported galaxy/absorber associations have $|\delta v| \leqslant 250\,\mathrm{km\,s^{-1}}$ and that our

results would not change qualitatively if we adopted a value lower than 400 km s$^{-1}$. Similarly, increasing the $|\delta v|$ limit to 600 km s$^{-1}$ has no qualitative impact on the following results.

We examine the results with particular emphasis on the galaxy luminosity. These were derived from the apparent $R$-band magnitude, redshift, and spectral type (see Prochaska et al. 2011). Generally, we consider three luminosity intervals: (1) $L < 0.1\,L^*$, termed dwarf galaxies; (2) $0.1\,L^* < L < L^*$, termed sub-$L^*$ galaxies; and (3) $L > L^*$, termed $L^*$ galaxies. For these definitions, we adopt the $r$-band value for $L^*$ as measured from the Sloan Digital Sky Survey (SDSS) which corresponds to $z \approx 0.1$: $r^* = -20.44 + 5\log h_{100}$ (Blanton et al. 2003). With the cosmology we have adopted, this yields $r^* = -21.12$ mag. We are motivated to this approach by the expectation that galaxies of a similar luminosity will, on average, trace similar environments and have dark matter halos with common characteristics. Ideally, we might separate the galaxies by their dark matter halo mass, as inferred from the galaxy's kinematics. Unfortunately, our spectra are of insufficient quality to discriminate on kinematics, nor do we have the necessary photometry to estimate stellar masses. Regarding the galaxy spectral type, we do make the distinction between early-type (absorption-line dominated) and late-type (emission-line dominated) galaxies based on our spectra (see Prochaska et al. 2011 for more details).

When discussing the results, we make a crude distinction between the virialized halo of a galaxy defined by a virial radius $r_{\rm vir}$ and the circumgalactic medium (CGM) that surrounds it to a larger radius $r_{\rm CGM}$. The motivation for this distinction is that galactic-scale processes (e.g., accretion, shock heating, outflows) may be especially active within the virialized halo, and therefore produce a medium that is qualitatively different from the surrounding CGM. Furthermore gas at $r < r_{\rm vir}$ may have a much greater probability of being gravitationally bound to the galaxy. At the same time, we doubt that $r_{\rm vir}$ marks a sharp boundary of any sort. Lastly, we note that a sight line which penetrates a galactic halo may show absorption from the gas within it and the CGM that surrounds it.

In standard numerical and analytic analysis, $r_{\rm vir}$ is predicted to scale with the dark matter halo mass as $r_{\rm vir} \propto M_h^{1/3}$ and with the circular velocity as $r_{\rm vir} \propto v_c$. If we were to adopt the observed $R$-band Tully–Fisher (TF) relation $L \propto v_c^{3.4}$ (Courteau et al. 2007), we would infer that $r_{\rm vir}$ scales as $r_{\rm vir} \propto L^{0.3}$. More modern treatments compare the clustering of galaxies as a function of luminosity to predictions for dark matter halos and thereby derive a relation between $L$ and $M_h$ (e.g., Zheng et al. 2007; Zehavi et al. 2011). These results, which are dominated by $L > L^*$ galaxies, imply $M_h \propto L^{3.8}$ (in $R$ band) at high luminosity and a much flatter relation at low luminosity (consistent with the higher $M/L$ ratio inferred for low-mass galaxies). Therefore, while most treatments—empirical and theoretical—tend to agree that $r_{\rm vir} \approx 250$–$300$ kpc for an $L^*$ galaxy, various prescriptions yield very different estimates for the virial radius of low-luminosity galaxies. In the following, we adopt characteristic values of $r_{\rm vir} \approx 100$ kpc for the dwarf galaxies, $r_{\rm vir} \approx 160$ kpc for a sub-$L^*$ galaxy, and $r_{\rm vir} \approx 250$ kpc for an $L^*$ galaxy. This corresponds to a scaling relation

$$r_{\rm vir} = r^*_{\rm vir}\left(\frac{L}{L^*}\right)^{\beta} \quad (1)$$

with $r^*_{\rm vir} = 250$ kpc and $\beta = 0.2$. These assignments and this relation are crude estimates and primarily serve to guide the discussion.

### 3.1. Gas Associated with Galaxies at Low Impact Parameter

In this subsection, we address the following question: granted that a galaxy with a certain luminosity lies at a given impact parameter from a quasar sight line, what is the probability of detecting Ly$\alpha$ or O VI absorption at that same redshift (within a given velocity interval $\delta v$) to a given equivalent width limit? More generally, we consider the distribution of equivalent widths and ionic column densities as a function of the galaxy luminosity $L$ and impact parameter $\rho$. In principle, such measurements reveal the physical conditions of gas in the virialized halos of galaxies and in the CGM that surrounds them (e.g., filaments, the intragroup medium). In turn, the measurements may inform whether the gas is physically connected to the galaxy (e.g., gravitationally bound to its dark matter halo) and/or which galaxies may "produce" IGM absorption at specific equivalent widths and column density.

There is (at least) one significant challenge to this analysis: galaxies cluster with one another. Therefore, if a galaxy lies at close impact parameter to a sight line there is a significant probability that one or more additional galaxies will also lie close to the same sight line. If we then detect IGM absorption at that redshift, there is an ambiguous association between the gas and each galaxy. One may be able to design an experiment that studied only isolated galaxies, but this would likely be unrepresentative of the full galaxy population. This issue is further complicated by the imperfections of our LCO/WFCCD survey. These include (1) the magnitude limit which implies sensitivity to fainter galaxies only at lower redshifts, (2) the limited field-of-view which precludes a search for galaxies with $\rho > 100$ kpc at the lowest redshifts, and (3) the varying sensitivity of the UV spectrometers with wavelength which dictates the equivalent width limit to Ly$\alpha$ and O VI absorption as a function of redshift. In the following, we emphasize these limitations where appropriate.

To (partially) address the ambiguity of multiple galaxies at a given redshift,[7] we perform the analysis separately for dwarf, sub-$L^*$, and $L^*$ galaxies. Initially, we examine all galaxies at impact parameter $\rho < 300$ kpc from the sight lines. This distance was arbitrarily chosen to exceed the virial radius of the galaxies yet to be small enough to primarily focus the analysis on individual galaxies. When two or more galaxies are separated by $|\delta v| < 400$ km s$^{-1}$ and have similar luminosity, we only present the one closest to the sight line (this occurs very rarely).

*Dwarf galaxies.* Consider first the $L < 0.1\,L^*$ galaxies (aka the dwarf galaxies); Table 3 lists the sample of systems at low impact parameter from our WFCCD survey. The table also lists the strongest Ly$\alpha$ and O VI absorbers within $|\delta v| \leqslant 400$ km s$^{-1}$ of each galaxy,[8] or an upper limit to the equivalent width and column density for non-detections. We also tabulate the closest galaxy with $L > 0.1\,L^*$ if one (or more) lies within 300 km s$^{-1}$ of the dwarf galaxy's redshift and 200 kpc of the sight line.

Figure 1 summarizes the absorption characteristics of the sample as a function of impact parameter. Regarding H I absorption, we note the positive detection of Ly$\alpha$ absorption for 14/16 (88%) of the galaxies to $W^{\rm Ly\alpha} = 100$ mÅ or $N_{\rm H\,I} = 10^{13.5}$ cm$^{-2}$.

[7] Previous authors have introduced criteria based on galaxy clustering to select the galaxy of interest when two or more with similar redshift are located near the sight line (Chen et al. 2001b). In general, this amounts to selecting the galaxy with smallest impact parameter (Morris & Jannuzi 2006).

[8] In response to the referee and following the publication of Paper IV, we have compared the redshifts of our LCO survey against those galaxies observed spectroscopically by SDSS. We find a mean velocity offset of $-30$ km s$^{-1}$ with a dispersion of 50 km s$^{-1}$ that is small compared to our velocity criterion.

**Table 3**
Dwarf Galaxies within 300 kpc of a QSO Sight Line

| Field | R.A. (J2000) | Decl. (J2000) | $z_{gal}$ | Type[a] | $\rho$ (kpc) | $L$ ($L^*$) | $z_{abs}^{Ly\alpha}$ | $W^{Ly\alpha}$ (mÅ) | $N_{H\,I}$ | Ref. | $z_{abs}^{O\,VI}$ | $W^{O\,VI}$ (mÅ) | $N_{O\,VI}$ | Ref. | $\rho_n$[b] | $L_n$[b] ($L^*$) |
|---|---|---|---|---|---|---|---|---|---|---|---|---|---|---|---|---|
| Q0026+1259 | 00:29:09.32 | +13:16:28.5 | 0.0329 | Late | 45 | 0.019 | ... | ... | ... | ... | 0.0329 | <120 | <14.00 | 9 | ... | ... |
| TONS180 | 00:57:04.01 | −22:26:51.2 | 0.0234 | Late | 154 | 0.021 | 0.0234 | 222 | 13.80 | 5 | 0.0234 | 43 | 13.48 | 4 | ... | ... |
| PKS0405−123 | 04:07:48.29 | −12:11:01.9 | 0.1670 | Late | 97 | 0.088 | 0.1671 | 697 | 15.47 | 3 | 0.1669 | 412 | 14.64 | 1 | 121 | 2.35 |
| PG1004+130 | 10:07:06.53 | +12:53:51.7 | 0.0092 | Late | 76 | 0.007 | 0.0092 | 260 | 13.90 | 9 | 0.0092 | <50 | <13.60 | 9 | ... | ... |
| | 10:07:30.77 | +12:53:50.0 | 0.0297 | Late | 174 | 0.055 | ... | ... | ... | ... | 0.0301 | <200 | <14.50 | 9 | ... | ... |
| HE1029−140 | 10:31:41.40 | −14:12:49.2 | 0.0508 | Early | 299 | 0.036 | 0.0516 | 278 | 14.00 | 5 | ... | ... | ... | ... | ... | ... |
| PG1116+215 | 11:19:03.14 | +21:16:23.4 | 0.0594 | Early | 216 | 0.026 | 0.0593 | 187 | 13.64 | 1 | 0.0593 | 63 | 13.77 | 1 | 130 | 0.11 |
| PG1211+143 | 12:14:06.93 | +14:04:38.3 | 0.0520 | Late | 180 | 0.097 | 0.0510 | 703 | 15.67 | 3 | 0.0513 | ... | 14.30 | 4 | 136 | 0.90 |
| | 12:14:13.92 | +14:03:31.0 | 0.0646 | Late | 71 | 0.092 | 0.0645 | 535 | 15.73 | 3 | 0.0645 | 144 | 14.16 | 3 | 147 | 0.81 |
| PG1216+069 | 12:18:38.69 | +06:42:29.3 | 0.0067 | Early | 89 | 0.032 | 0.0063 | 2320 | 19.30 | 7 | 0.0063 | <200 | <14.20 | 9 | ... | ... |
| | 12:19:20.68 | +06:42:18.9 | 0.0081 | Early | 35 | 0.009 | 0.0081 | <60 | <13.10 | 9 | 0.0081 | <200 | <14.20 | 9 | ... | ... |
| | 12:19:03.75 | +06:33:43.2 | 0.0132 | Early | 102 | 0.015 | 0.0126 | 288 | 13.94 | 6 | 0.0126 | <200 | <14.20 | 9 | ... | ... |
| 3C273 | 12:29:50.58 | +02:01:54.3 | 0.0062 | Early | 82 | 0.006 | 0.0053 | 365 | 15.38 | 3 | 0.0053 | <15 | <13.17 | 4 | ... | ... |
| MRK1383 | 14:29:42.43 | +01:17:50.9 | 0.0281 | Early | 297 | 0.010 | 0.0282 | 225 | 13.67 | 3 | 0.0283 | <16 | <13.10 | 4 | ... | ... |
| | 14:28:58.43 | +01:13:05.5 | 0.0299 | Late | 156 | 0.025 | 0.0299 | 66 | 13.10 | 5 | 0.0299 | <40 | <13.50 | 9 | ... | ... |
| FJ2155-0922 | 21:54:56.82 | −09:27:24.2 | 0.0504 | Early | 294 | 0.049 | 0.0515 | 272 | 14.08 | 3 | 0.0501 | <68 | <13.91 | 4 | ... | ... |
| | 21:54:52.29 | −09:24:37.5 | 0.0808 | Early | 284 | 0.077 | 0.0808 | 1007 | 15.11 | 3 | 0.0807 | <14 | <13.06 | 4 | 34 | 0.95 |
| PKS2155−304 | 21:58:30.50 | −30:11:02.0 | 0.0169 | Early | 117 | 0.002 | 0.0170 | 143 | 13.56 | 3 | 0.0167 | <15 | <12.99 | 4 | ... | ... |

**Notes.** Upper limits correspond to $2\sigma$ constraints.
[a] Spectral type (see the text for the quantitative definition).
[b] Impact parameter and luminosity of the brightest galaxy ($L > 0.1\,L^*$) within 200 kpc and $|\delta v| < 400\,km\,s^{-1}$ (if any).
**References.** (1) Tripp et al. 2008; (2) Thom & Chen 2008b; (3) Danforth & Shull 2008; (4) Danforth et al. 2006; (5) Penton et al. 2004; (6) Chen & Mulchaey 2009; (7) Tripp et al. 2005; (9) this paper.

We emphasize that unlike the high-$z$ universe where the Ly$\alpha$ forest is sufficiently "dense" that one identifies a line every $\sim$100 km s$^{-1}$, the probability of randomly associating a galaxy with an absorber is small at $z \sim 0$. Taking PG1116+215 as a representative sight line, the Ly$\alpha$ lines reported by Danforth & Shull (2008) cover $\approx$33% of the sight line for $|\delta v| < 400\,km\,s^{-1}$ to $N_{H\,I} \approx 10^{13}\,cm^{-2}$. Restricting to Ly$\alpha$ lines with $N_{H\,I} \geqslant 10^{13.5}\,cm^{-2}$ (Figure 1), which is more characteristic of the gas associated with the dwarf galaxies, we find that only $\approx$10% of the sight line is covered. As such, if we randomly assigned redshifts to the galaxies with values uniformly sampling $z = [0, z_{em}]$, the probability of recovering 14/16 associations with Ly$\alpha$ lines having $N_{H\,I} > 10^{13.5}\,cm^{-2}$ is negligible. We conclude, therefore, that Ly$\alpha$ absorption traces dwarf galaxies to impact parameters of 300 kpc or greater with a nearly unit covering fraction to $W^{Ly\alpha} = 100$ mÅ ($N_{H\,I} = 10^{13.5}\,cm^{-2}$).

Inspecting Figure 1 we note that the majority of dwarf-galaxy–Ly$\alpha$ associations are at an impact parameter that is well beyond the presumed virial radius of $r_{vir} \approx 100$ kpc. We infer, therefore, that the connection between these galaxies and H I absorption is not driven by galactic-scale phenomena, e.g., tidal debris, accreting gas, outflows; H I gas also arises in the extended CGM of these galaxies. The direct implication is that the two phenomena (Ly$\alpha$ absorption and dwarf galaxies) are simply highly correlated tracers of the same large-scale overdensity in the universe (e.g., a filament). This assertion is further supported by the fact that there is no strong correlation between the impact parameter and the Ly$\alpha$ absorption (in column density or equivalent width).

It is also evident from Figure 1 that a subset of the dwarf galaxies are associated with relatively strong Ly$\alpha$ absorbers, $W^{Ly\alpha} > 0.5$ Å and $N_{H\,I} > 10^{15}\,cm^{-2}$. However, most of these strong absorbers may also be associated with a brighter galaxy ($L > 0.1\,L^*$) within 200 kpc of the sight line. We have overplotted on the points gray boxes (diamonds) to indicate dwarf galaxies where an additional sub-$L^*$ ($L^*$) galaxy lies within 150 kpc of the sight line. With the exception of the two galaxies associated with Virgo (at $z \approx 0.006$ toward PG1216+069 and 3C273; marked with gray triangles), all of the dwarf galaxies with associated strong Ly$\alpha$ absorption also have a brighter galaxy near the sight line. Furthermore, there are no cases where a brighter galaxy is nearby and the Ly$\alpha$ equivalent width is low. Although limited by small number statistics, these results suggest that the strongest H I absorbers are preferentially associated with an $L > 0.1\,L^*$ galaxy instead of the dwarf.

Lastly, with regards to dwarf galaxies and H I absorption, we consider the two non-detections in Ly$\alpha$. One case is located at nearly 300 kpc from PKS1302–102 and we may dismiss it because of the large impact parameter. The other example, however, is for a $z = 0.0081$ early-type galaxy[9] that has the lowest impact parameter ($\rho = 34$ kpc) of the entire sample! Furthermore, it is the only example we have where the sight line is certain to intersect the galaxy's virialized halo. We identify no other galaxies at this redshift and only note that it might be associated with the extreme outskirts of Virgo. Either way, this non-detection stresses that the IGM/galaxy connection shows special cases that contradict dominant trends.

The lower panels of Figure 1 present the equivalent width of O VI 1031 ($W^{1031}$; when UV spectral coverage exists) and an estimate of the $O^{+5}$ column density $N_{O\,VI}$ for the strongest absorber within 300 km s$^{-1}$ of each galaxy. In contrast to Ly$\alpha$, the results are dominated by non-detections. Furthermore, four of five systems with a positive detection (3/4 for those with $N_{O\,VI} > 10^{14}\,cm^{-2}$) also show a brighter galaxy ($L > 0.1\,L^*$) within 150 kpc of the sight line. Ignoring these systems, 0/13 of "isolated" dwarf galaxies show a positive detection to an equivalent width limit of 200 mÅ and only 2/8 for a

[9] The SDSS survey reports a redshift $z = 0.0074 \pm 0.0003$ for this galaxy based on a low S/N spectrum with weak spectral features.

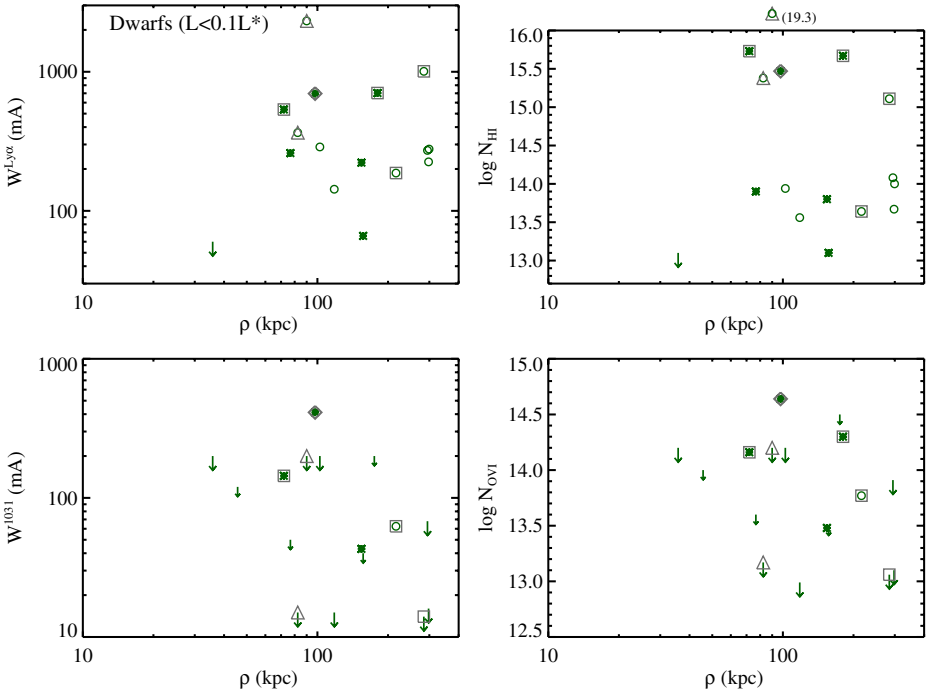


**Figure 1.** Four panels show the measured equivalent widths and column densities of Ly$\alpha$ and O VI absorption for all of the dwarf galaxies ($L < 0.1\,L^*$) in our LCO/WFCCD survey that lie within 300 kpc of a quasar sight line (where high-quality UV spectroscopy exists). In each case, we report the maximum value for all Ly$\alpha$ (or O VI) absorption lines detected within 400 km s$^{-1}$ of the galaxy redshift. Asterisks denote galaxies with late-type spectra and open circles denote early-type spectra (small/large arrows indicated limits for late/early-type galaxies). In cases where there is more than one dwarf galaxy within 400 km s$^{-1}$ of one another, we plot only the one closest to the sight line. Upper limits denote non-detections or, in a few cases, unresolved blends with coincident absorption lines. The gray boxes (diamonds) denote systems where an additional sub-$L^*$ ($L^*$) galaxy lies within 150 kpc of the sight line. Remarkably, these include nearly all of the systems associated with strong Ly$\alpha$ absorption and positive O VI detections. The gray triangles, meanwhile, denote galaxies associated with Virgo. This includes the system at $z = 0.063$ toward PG1216+069 which falls beyond the $N_{\rm H\,I}$ axes in the upper, right panel (labeled with its $N_{\rm H\,I}$ value). Note the preponderance of Ly$\alpha$ associations but the rare detection of O VI gas, especially if one ignores the dwarf galaxies with a brighter neighbor near the sight line.

(A color version of this figure is available in the online journal.)

50 mÅ limit. We conclude that the CGM of dwarf galaxies at impact parameters of 50–300 kpc rarely shows O VI absorption characteristic of current UV surveys. The CGM of dwarf galaxies does give rise to nearly ubiquitous H I absorption, but has insufficient surface density, metallicity, and/or the physical conditions (i.e., density, temperature) needed to also exhibit significant O VI absorption.

In summary, the CGM of dwarf galaxies at $\rho \gtrsim 100$ kpc is characterized by a high incidence of moderate strength Ly$\alpha$ absorption ($W^{\rm Ly\alpha} \gtrsim 200$ mÅ) and a low incidence of O VI absorption to modest equivalent width limits. Our survey, unfortunately, offers few probes of dwarf galaxies on smaller scales, i.e., with sight lines intersecting their dark matter halos. This assessment awaits a dedicated survey of such galaxies.[10]

*$L^*$ galaxies*. In Figure 2, we plot the same quantities versus impact parameter but now for $L > L*$ galaxies (Table 4). Our survey has only a modest sample of such bright galaxies within 300 kpc of the sight lines which reflects, of course, their lower comoving number density. Similar to the dwarf galaxies, nearly every $L^*$ galaxy exhibits significant Ly$\alpha$ absorption.[11] This even includes luminous, early-type galaxies which are likely gas-poor on galactic scales. The average equivalent width at $\rho = 100$–$200$ kpc is $W^{\rm Ly\alpha} \approx 500$ mÅ and ≈400 mÅ at $\rho = 200$–$300$ kpc, twice that observed for the dwarf galaxies (ignoring dwarfs with bright neighbors; Table 3). Similarly, the $N_{\rm H\,I}$ values of the $L^*$ galaxies exceed those for the dwarfs. This implies that the H I gas near a typical $L^*$ galaxy has a higher total surface density, neutral fraction, and/or a more extreme velocity field. Such trends with luminosity have been revealed previously (e.g., Chen et al. 2001b); presumably, they are a simple consequence of these galaxies having greater mass.

Regarding O VI absorption, the $L^*$ galaxies show a greater fraction (5/10) of positive detections than dwarf galaxies. Furthermore, there is a possible trend with impact parameter: all of the detections occur within $\rho = 225$ kpc, which corresponds (roughly) to the virial radii of these luminous galaxies. The figure also reveals that every emission-line galaxy exhibits a positive O VI detection; all of the non-detections are associated with early-type spectra. A preference for O VI absorption to occur in late-type galaxies was previously reported by Chen & Mulchaey (2009) for their modest sample of galaxy/O VI associations (Tumlinson et al. 2011). Unfortunately, all of our non-detections also occur at large $\rho$ and, therefore, we cannot separate the effects of impact parameter and spectral type with this sample. Nevertheless, the results demonstrate clearly that the extended CGM of $L^*$ galaxies (at least those with early-type spectra) is frequently characterized by the non-detection of O VI gas.

*Sub-$L^*$ galaxies*. Our final galaxy subset is the sub-$L^*$ galaxies ($0.1\,L^* < L < L^*$; Table 5). Figure 3 reveals a 100% detection rate for H I gas to $\rho = 300$ kpc for these galaxies. In contrast to the other galaxy subsets, the Ly$\alpha$ equivalent widths of the sub-$L^*$ galaxies show a very obvious trend with impact

[10] An ongoing Cycle 18 *HST*/COS survey by J. Tumlinson (GO 12248) is designed to address this directly, although it will not include high S/N spectra of the O VI doublet.

[11] The only notable exception is an $L \approx 1.0\,L*$ galaxy with an early-type spectrum located at an impact parameter of $\rho \approx 250$ kpc from PKS0405–123 ($z = 0.203$). Perhaps not coincidentally, it also is associated with one of the most significant galaxy overdensities identified in our survey.

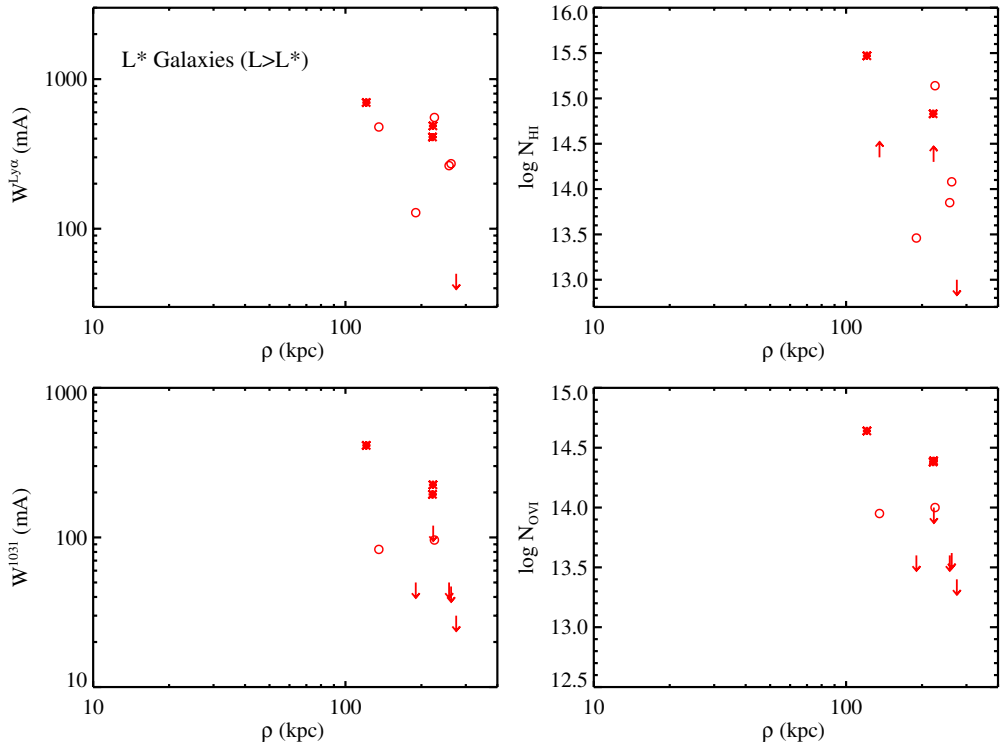


**Figure 2.** Same as Figure 1 but for $L^*$ galaxies. Note the high covering fraction to Ly$\alpha$ absorption (with column densities typically exceeding $10^{14}$ cm$^{-2}$) but the lack of O VI detections for $\rho > 225$ kpc to sensitive limits. The results suggest that O VI gas near $L^*$ galaxies is primarily associated with their virialized halos but not their extended CGM environments.

(A color version of this figure is available in the online journal.)

**Table 4**
$L > L^*$ Galaxies within 300 kpc of a QSO Sight Line

| Field | R.A. (J2000) | Decl. (J2000) | $z_{\rm gal}$ | Type[a] | $\rho$ (kpc) | $L$ ($L^*$) | $\mathcal{N}$[b] | $z_{\rm abs}^{\rm Ly\alpha}$ | $W^{\rm Ly\alpha}$ (mÅ) | $N_{\rm H\,I}$ | Ref. | $z_{\rm abs}^{\rm O\,VI}$ | $W^{\rm O\,VI}$ (mÅ) | $N_{\rm O\,VI}$ | Ref. |
|---|---|---|---|---|---|---|---|---|---|---|---|---|---|---|---|
| Q0026+1259 | 00:29:15.36 | +13:20:57.0 | 0.0393 | Early | 222 | 1.505 | 0 | ... | ... | ... | ... | 0.0393 | <120 | <14.00 | 9 |
| PKS0405−123 | 04:07:44.03 | −12:12:09.5 | 0.1532 | Early | 189 | 1.073 | 1 | 0.1522 | 128 | 13.46 | 3 | 0.1522 | <50 | <13.60 | 9 |
| | 04:07:51.28 | −12:11:38.3 | 0.1670 | Late | 120 | 2.349 | 1 | 0.1671 | 697 | 15.47 | 3 | 0.1669 | 412 | 14.64 | 1 |
| | 04:07:42.79 | −12:11:33.1 | 0.2030 | Early | 274 | 1.175 | 9 | 0.2030 | <50 | <13.00 | 9 | 0.2030 | <30 | <13.40 | 9 |
| | 04:07:50.69 | −12:12:25.2 | 0.2976 | Early | 257 | 2.074 | 7 | 0.2977 | 264 | 13.85 | 3 | 0.2976 | <50 | <13.60 | 9 |
| | 04:07:45.96 | −12:11:09.9 | 0.3612 | Early | 225 | 7.318 | 5 | 0.3608 | 554 | 15.14 | 3 | 0.3616 | 96 | 14.00 | 1 |
| PG1116+215 | 11:19:06.73 | +21:18:29.3 | 0.1383 | Early | 135 | 2.231 | 4 | 0.1385 | 479 | >14.35 | 1 | 0.1385 | 83 | 13.95 | 1 |
| PKS1302−102 | 13:05:20.22 | −10:36:30.4 | 0.0426 | Late | 221 | 2.804 | 1 | 0.0422 | 410 | 14.83 | 3 | 0.0422 | 194 | 14.38 | 3 |
| FJ2155−0922 | 21:54:56.64 | −09:18:07.9 | 0.0517 | Early | 262 | 1.553 | 0 | 0.0515 | 272 | 14.08 | 3 | 0.0514 | <47 | <13.62 | 4 |
| | 21:55:06.53 | −09:23:25.2 | 0.1326 | Late | 222 | 1.779 | 2 | 0.1324 | 487 | <14.30 | 1 | 0.1324 | 225 | 14.39 | 1 |

**Notes.**
[a] Spectral type (see the text for the quantitative definition).
[b] Number of additional galaxies within 3 Mpc of the sight line, 400 km s$^{-1}$ of this galaxy, and having $L > 0.1\,L^*$.
**References.** (1) Tripp et al. 2008; (2) Thom & Chen 2008b; (3) Danforth & Shull 2008; (4) Danforth et al. 2006; (5) Penton et al. 2004; (6) Chen & Mulchaey 2009; (9) this paper.

parameter. A Spearman's test reports that the null hypothesis of no correlation is ruled out at >99.5% c.l. There is also the hint of a division in the $W^{\rm Ly\alpha}$ values at $\rho \approx 100$ kpc, i.e., between exclusively large equivalent widths ($W^{\rm Ly\alpha} > 1$ Å for $\rho < 100$ kpc) and a large scatter of primarily lower values for $\rho > 100$ kpc (Table 6). As this impact parameter roughly coincides with the virial radius expected for sub-$L^*$ galaxies, if confirmed, it may be related to galactic-scale processes at $\rho < r_{\rm vir}$ whereas the $W^{\rm Ly\alpha}$ values at larger $\rho$ trace the physical properties of the surrounding (unvirialized) CGM.

Because the Ly$\alpha$ line is saturated for most of the systems, the $W^{\rm Ly\alpha}$ values are a good proxy for kinematics, i.e., the systems at $\rho < 100$ kpc require a velocity spread of $\Delta v = cW^{\rm Ly\alpha}/(1215.67\,\text{Å}) \approx 250\,{\rm km\,s^{-1}}({\rm W^{Ly\alpha}}/1\,\text{Å})$. Such motions may be just consistent with galaxies having circular velocities $v_c \gtrsim 100\,{\rm km\,s^{-1}}$, a reasonable estimate for sub-$L^*$ galaxies. There is also the hint of a difference in Ly$\alpha$ equivalent width for galaxies with differing spectral type: the late-type galaxies have systematically higher $W^{\rm Ly\alpha}$ values than early-type galaxies at a similar impact parameter. This conclusion is tempered, however,

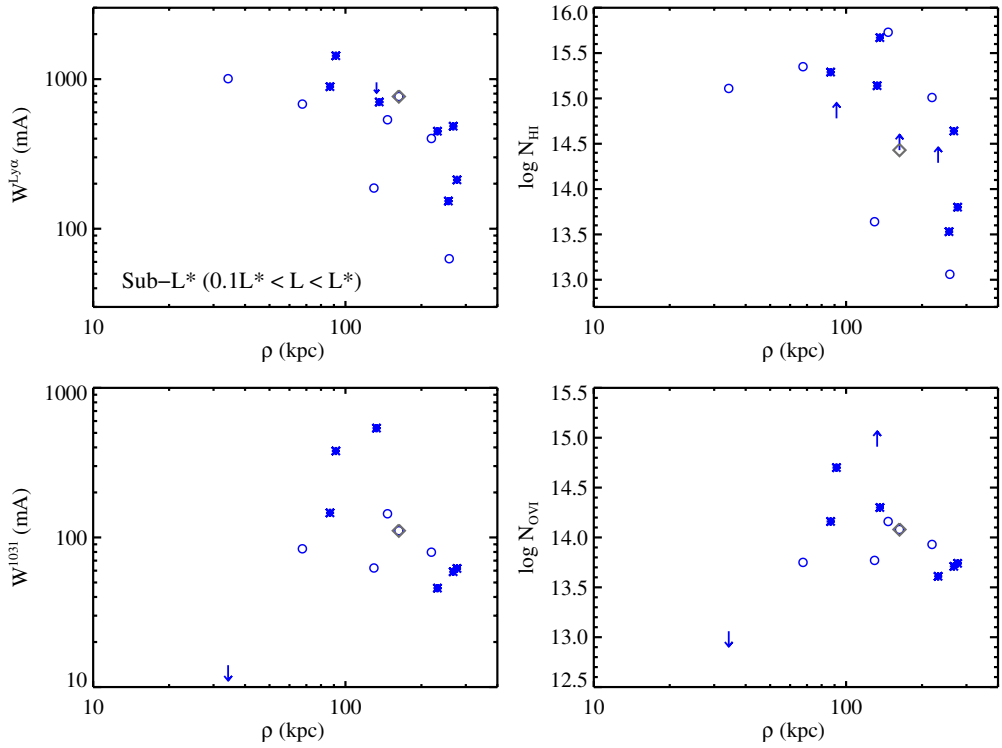


**Figure 3.** Same as Figure 1 but for sub-$L^*$ galaxies. One notes a strong correlation between $W^{\rm Ly\alpha}$ and impact parameter for these galaxies and also an apparent division at $\rho \approx 100$ kpc between $W^{\rm Ly\alpha} \gtrsim 1$ Å and lines exhibiting a large scatter of lower values. Intriguingly, this division occurs near the expected virial radius for these galaxies. In contrast to the dwarf and $L^*$ galaxies (Figures 1 and 2), we observe a very high detection rate for O VI at all impact parameters. This indicates that the extended CGM of sub-$L^*$ galaxies has a high covering fraction to modest O VI absorption. The gray diamond indicates the one sub-$L^*$ galaxy in our sample that has an $L^*$ neighbor within 150 kpc of the sight line.

(A color version of this figure is available in the online journal.)

**Table 5**
Sub-$L^*$ Galaxies ($0.1\,L^* < L < L^*$) within 300 kpc of a QSO Sight Line

| Field | R.A. (J2000) | Decl. (J2000) | $z_{\rm gal}$ | Type[a] | $\rho$ (kpc) | $L$ ($L^*$) | $\mathcal{N}$[b] | $z_{\rm abs}^{\rm Ly\alpha}$ | $W^{\rm Ly\alpha}$ (mÅ) | $N_{\rm H\,I}$ | Ref. | $z_{\rm abs}^{\rm O\,VI}$ | $W^{\rm O\,VI}$ (mÅ) | $N_{\rm O\,VI}$ | Ref. |
|---|---|---|---|---|---|---|---|---|---|---|---|---|---|---|---|
| TONS180 | 00:57:08.52 | −22:18:29.6 | 0.0456 | Late | 276 | 0.397 | 1 | 0.0456 | 212 | 13.80 | 5 | 0.0456 | 62 | 13.74 | 4 |
| PKS0312−77 | 03:12:01.76 | −76:55:17.7 | 0.0594 | Late | 255 | 0.318 | 0 | 0.0595 | 153 | 13.53 | 3 | ... | ... | ... | ... |
| | 03:11:57.89 | −76:51:55.6 | 0.2026 | Late | 132 | 0.696 | 2 | 0.2027 | <952 | 15.14 | 3 | 0.2027 | 538 | >14.91 | 1 |
| PKS0405−123 | 04:07:58.12 | −12:12:24.7 | 0.0965 | Late | 267 | 0.164 | 8 | 0.0966 | 484 | 14.64 | 3 | 0.0966 | 59 | 13.71 | 3 |
| | 04:07:48.40 | −12:12:10.8 | 0.3520 | Unkn | 165 | 0.302 | 2 | 0.3509 | 380 | 14.04 | 3 | 0.3509 | 24 | 13.35 | 3 |
| PG1116+215 | 11:19:05.55 | +21:17:33.3 | 0.0600 | Early | 129 | 0.113 | 5 | 0.0593 | 187 | 13.64 | 1 | 0.0593 | 63 | 13.77 | 1 |
| | 11:19:12.20 | +21:18:52.0 | 0.1660 | Early | 162 | 0.369 | 15 | 0.1655 | 765 | >14.43 | 1 | 0.1655 | 111 | 14.08 | 1 |
| PG1211+143 | 12:14:09.54 | +14:04:21.3 | 0.0511 | Late | 136 | 0.902 | 8 | 0.0510 | 703 | 15.67 | 3 | 0.0513 | ... | 14.30 | 4 |
| | 12:14:19.86 | +14:05:10.3 | 0.0644 | Early | 146 | 0.806 | 0 | 0.0645 | 535 | 15.73 | 3 | 0.0645 | 144 | 14.16 | 3 |
| PG1216+069 | 12:19:23.45 | +06:38:20.3 | 0.1241 | Late | 91 | 0.711 | 6 | 0.1236 | 1433 | >14.78 | 1 | 0.1236 | 378 | 14.70 | 1 |
| PKS1302−102 | 13:05:32.19 | −10:33:56.9 | 0.0936 | Early | 67 | 0.213 | 7 | 0.0949 | 681 | 15.35 | 3 | 0.0948 | 84 | 13.75 | 4 |
| | 13:05:35.30 | −10:33:24.2 | 0.1453 | Late | 86 | 0.433 | 2 | 0.1453 | 890 | 15.29 | 3 | 0.1453 | 146 | 14.16 | 4 |
| | 13:05:34.97 | −10:34:22.6 | 0.1917 | Early | 219 | 0.974 | 2 | 0.1916 | 401 | 15.01 | 3 | 0.1916 | 80 | 13.93 | 1 |
| FJ2155−0922 | 21:54:50.87 | −09:22:33.3 | 0.0788 | Late | 231 | 0.172 | 22 | 0.0777 | 448 | >14.29 | 1 | 0.0777 | 46 | 13.61 | 1 |
| | 21:54:59.96 | −09:22:24.7 | 0.0810 | Early | 34 | 0.950 | 10 | 0.0808 | 1007 | 15.11 | 3 | 0.0807 | <14 | <13.06 | 4 |
| | 21:55:01.62 | −09:20:47.0 | 0.1555 | Early | 257 | 0.483 | 1 | 0.1549 | 63 | 13.06 | 3 | ... | ... | ... | ... |

**Notes.**
[a] Spectral type (see the text for the quantitative definition).
[b] Number of additional galaxies within 3 Mpc of the sight line, 400 km s$^{-1}$ of this galaxy, and having $L > 0.1\,L^*$.
**References.** (1) Tripp et al. 2008; (2) Thom & Chen 2008b; (3) Danforth & Shull 2008; (4) Danforth et al. 2006; (5) Penton et al. 2004; (6) Chen & Mulchaey 2009; (9) this paper.

by the relatively small sample size and should be confirmed with a larger data set.

Remarkably, the sub-$L^*$ galaxies show a very high incidence of associated O VI absorption for impact parameters $\rho < 300$ kpc. At $\rho < 100$ kpc, 3/4 (75%) of the galaxies have $W^{1031} > 50$ mÅ ($N_{\rm O\,VI} > 10^{13.5}$ cm$^{-2}$). And at larger impact parameters, the incidence is yet higher. It appears that the association extends well beyond the virial radii of these galaxies;

**Table 6**
Galaxy/Absorber Statistics

| Luminosity | $\rho$ (kpc) | $\mathcal{N}_{\rm gal}$ | Med($W^{\rm Ly\alpha}$) (Å) | rms($W^{\rm Ly\alpha}$) (Å) | $\mathcal{N}_{\rm gal}$ | Med($N_{\rm H\,I}$) | rms($N_{\rm H\,I}$) | $\mathcal{N}_{\rm gal}$ | Med($W^{1031}$) (mÅ) | rms($W^{1031}$) (mÅ) | $\mathcal{N}_{\rm gal}$ | Med($N_{\rm O\,VI}$) | rms($N_{\rm O\,VI}$) |
|---|---|---|---|---|---|---|---|---|---|---|---|---|---|
| $L < 0.1\,L^*$ | | | | | | | | | | | | | |
| | 0–100 | 6 | 0.54 | 0.82 | 6 | 15.5 | 2.1 | 7 | <144 | 130 | 7 | <14.2 | 0.5 |
| | 100–200 | 5 | 0.22 | 0.25 | 5 | 13.8 | 1.0 | 5 | < 43 | 92 | 6 | <14.2 | 0.6 |
| | 200–300 | 5 | 0.27 | 0.34 | 5 | 14.0 | 0.6 | 4 | < 62 | 29 | 4 | <13.8 | 0.4 |
| $0.1 < L < L^*$ | | | | | | | | | | | | | |
| | 0–100 | 4 | 1.01 | 0.32 | 4 | 15.3 | 0.3 | 4 | 146 | 158 | 4 | 14.2 | 0.7 |
| | 100–200 | 6 | 0.70 | 0.28 | 6 | 15.1 | 0.9 | 5 | 111 | 207 | 6 | 14.2 | 0.5 |
| | 200–300 | 6 | 0.40 | 0.17 | 6 | 14.3 | 0.7 | 4 | 62 | 13 | 4 | 13.7 | 0.1 |
| $L > L^*$ | | | | | | | | | | | | | |
| | 100–200 | 3 | 0.48 | 0.29 | 3 | 14.4 | 1.0 | 3 | 83 | 200 | 3 | 13.9 | 0.5 |
| | 200–300 | 6 | 0.41 | 0.18 | 6 | 14.3 | 0.8 | 7 | <96 | 75 | 7 | <14.0 | 0.4 |
| All Galaxies | | | | | | | | | | | | | |
| | 0–100 | 10 | 0.70 | 0.66 | 10 | 15.4 | 1.6 | 11 | <144 | 132 | 11 | <14.2 | 0.5 |
| | 100–300 | 25 | 0.28 | 0.23 | 25 | 14.0 | 0.7 | 23 | <62 | 113 | 24 | <13.8 | 0.5 |
| | 300–500 | 31 | 0.16 | 0.15 | 30 | 13.7 | 0.7 | 19 | <44 | 37 | 22 | <13.6 | 0.4 |
| | 500–1000 | 41 | 0.06 | 0.16 | 40 | 13.1 | 0.8 | 18 | <50 | 33 | 19 | <13.6 | 0.3 |

**Note.** For column densities, all statistics are calculated on log $N$.

the results require that sub-$L^*$ galaxies are surrounded by a CGM that bears O VI gas to an impact parameter of several hundreds of kpc. We also emphasize that only one of the galaxies has a neighboring, bright ($L > L^*$) galaxy close to the sight line. Finally, we note a possible trend of decreasing $W^{1031}$ (and $N_{\rm O\,VI}$) with increasing impact parameter. This trend, however, is dominated by the two cases at $\rho \approx 100$ kpc with large $W^{1031}$ values.

The non-detection of O VI absorption for the galaxy at $z = 0.081$ and $\rho = 33$ kpc in the FJ2155–0922 field warrants additional discussion. It is striking, given the high incidence of O VI detections, that the galaxy at smallest impact parameter would exhibit the lowest $W^{1031}$ value.[12] Furthermore, as is evident from Figure 3 and Table 5, there is very strong Ly$\alpha$ absorption associated with this galaxy ($W^{\rm Ly\alpha} > 1$ Å). It has an early-type spectrum, and its luminosity places it at the upper end of the sub-$L^*$ population. It is noteworthy that this galaxy lies within an overdensity in the FJ2155–0922 field: 10 galaxies with $L > 0.1\,L^*$ lie within 3 Mpc of the sight line. On the other hand, the $z = 0.0788$, sub-$L^*$ galaxy ($\rho = 221$ kpc) in the same field has 22 such neighbors yet shows modest O VI absorption. Previous studies have reported similar 'peculiar" non-detections in regions of relatively high galaxy density (e.g., Tripp et al. 2002, 2005; Wakker & Savage 2009). Similar to the non-detection of Ly$\alpha$ at $\rho \approx 30$ kpc for the dwarf galaxy in the PG1216+069 field, this one non-detection of O VI gas stresses the complexity of galaxy/absorber associations.

In summary, all three classes of galaxies considered above exhibit high covering fractions to Ly$\alpha$ absorption for impact parameters $\rho < 300$ kpc. There are possible trends of increasing $W^{\rm Ly\alpha}$ values for brighter galaxies and decreasing $W^{\rm Ly\alpha}$ values at higher impact parameter. In contrast, the covering fraction to O VI absorption is highest for sub-$L^*$ galaxies, low for dwarf galaxies, and low for early-type (and/or high-$\rho$) $L^*$ galaxies. These results are empirical descriptions of the gas associated with low-$z$ galaxies; we explore further the implications for the origins of Ly$\alpha$ and O VI absorption in the following sections.

[12] We have confirmed the measurements of Danforth et al. (2006) by analyzing our extraction of the *FUSE* spectrum for FJ2155–0922.

### 3.2. Galaxies associated with IGM Absorption

In the previous sub-section, we studied the Ly$\alpha$ and O VI absorption associated with galaxies at low impact parameters to quasar sight lines. For that analysis, the measures (luminosity, impact parameter, equivalent width) were all well defined and the results were relatively insensitive to biases related to incompleteness in the galaxy survey. The key complication of such an analysis, however, is that galaxies cluster and therefore their environment (e.g., the presence of a brighter, nearby neighbor) may play a significant role in observed associations between a galaxy and the IGM. Furthermore, this approach only indirectly addresses fundamental questions related to the origin of Ly$\alpha$ and O VI gas in the IGM.

One may gain further insight by reversing the experiment, i.e., to study the properties of the closest (detected) galaxy to a given set of IGM absorption lines. In this manner, one tests how frequently galaxies and their halos are associated with various components of the IGM, and one may assess their physical properties and environment. This approach, however, has the obvious downside that no galaxy survey is truly complete, neither in terms of field-of-view nor depth. Indeed, our survey does not cover sufficient area to identify all galaxies within $\rho \approx 200$ kpc for $z < 0.02$ and our magnitude limit implies significant incompleteness to $L < 0.1\,L^*$ in most fields for $z > 0.1$. Therefore, we restrict the following analysis and discussion to the redshift interval $0.02 < z < 0.2$ and caution that at the high end we have limited sensitivity to very faint galaxies.

In Figure 4, we present the analysis for Ly$\alpha$ where the symbols label the luminosity of the closest galaxy detected and the upward arrows[13] indicate absorbers without an associated galaxy in our survey. For very low column densities, $10^{13}\,{\rm cm}^{-2} < N_{\rm H\,I} < 10^{14}\,{\rm cm}^{-2}$, approximately 40% of the absorbers may be associated with a galaxy within 1 Mpc, always at $\rho > 100$ kpc and primarily at $\rho > 200$ kpc (80% of the associations). We conclude that *few, if any, of the weak Ly$\alpha$ absorbers arise from the virialized halos of $z \sim 0$ galaxies*. Instead, weak

[13] These arrows are placed at the physical distance equivalent to 10′ angular separation (the typical field of view for the LCO/WFCCD survey) at the redshift of the absorber.

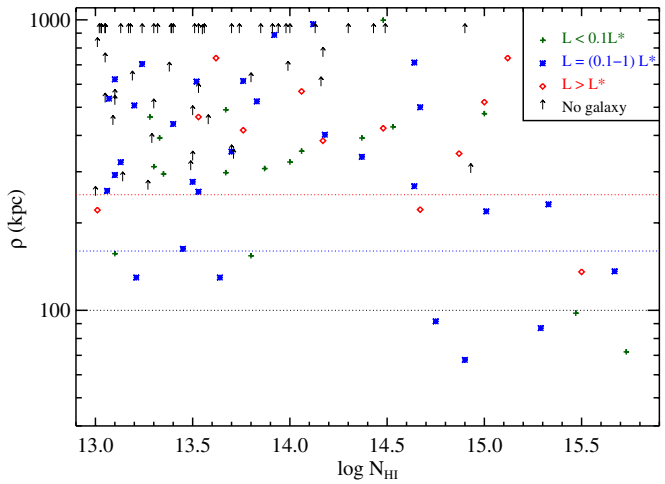


**Figure 4.** Impact parameter (symbols indicate luminosity) of the galaxy closest to the sight line with a redshift coincident ($|\delta v| < 400\,\mathrm{km\,s^{-1}}$) to the Ly$\alpha$ absorbers detected along our quasar sight lines. Note that most of the $N_{\rm H\,I}$ values exceeding $10^{14.5}\,\mathrm{cm^{-2}}$ should be considered lower limits due to line saturation. The dotted lines (from bottom to top) mark estimates for the virial radii of the dwarf, sub-$L^*$, and $L^*$ galaxies, respectively. In cases where we have not detected a galaxy within 1 Mpc of the sight line, we plot an upward arrow at the distance at each absorber's redshift corresponding to the typical $10'$ field of view for our LCO/WFCCD galaxy survey. For $N_{\rm H\,I} < 10^{14.5}\,\mathrm{cm^{-2}}$, the incidence of associated galaxies is low and those that are detected generally lie at $\rho > 200$ kpc. We conclude that few, if any, of these absorbers arise in the virialized halos of $z \sim 0$ galaxies. At higher column densities, the fraction of Ly$\alpha$ absorbers with an associated galaxy increases and the impact parameter to the systems decreases suggesting a physical association between the gas and galaxy.

(A color version of this figure is available in the online journal.)

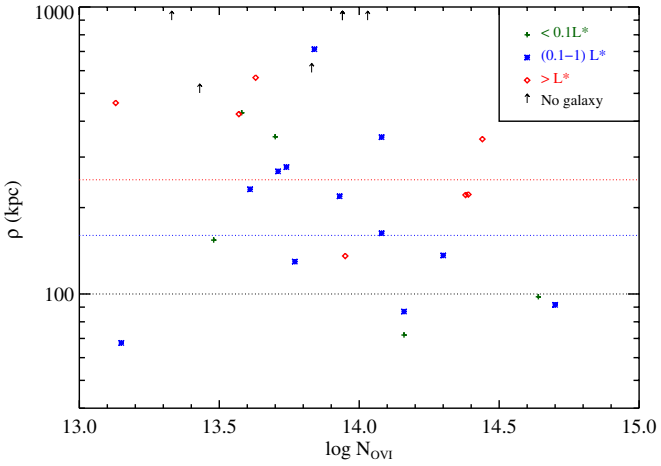


**Figure 5.** Impact parameter (symbols indicate luminosity) of the galaxy closest to the sight line with a redshift coincident ($|\delta v| < 400\,\mathrm{km\,s^{-1}}$) to the O VI absorbers detected along our quasar sight lines. The dotted horizontal lines mark estimates (from bottom to top) for the virial radii of the dwarf, sub-$L^*$, and $L^*$ galaxies, respectively. The arrows are positioned in Figure 4. One notes that although most of the O VI absorbers have an associated galaxy within a few hundred kpc of the sight line, very few of the sight lines intersect the galaxy's expected virialized halo. The results suggest that O VI gas is associated primarily with the extended CGM of $z \sim 0$ galaxies. There is possibly an anti-correlation between $\rho$ and $N_{\rm O\,VI}$, but the significance of such a trend is tempered by the large scatter.

(A color version of this figure is available in the online journal.)

H I absorption traces either the extended CGM of galaxies or, more commonly, structures with a low filling factor of galaxies (non-detections). The results are similar for the Ly$\alpha$ lines with modest $N_{\rm H\,I}$ ($10^{14}$–$10^{15}\,\mathrm{cm^{-2}}$), although the incidence of an association to a galaxy with $\rho < 1$ Mpc is higher (70%). For the small set of strong H I absorption lines ($N_{\rm H\,I} > 10^{15}\,\mathrm{cm^{-2}}$), the results are qualitatively different. Every Ly$\alpha$ line is linked to a galaxy and the majority of these have $\rho < 200$ kpc. Even in these cases, however, the association with a virialized halo may be tenuous. Altogether, our results do offer further evidence that large $N_{\rm H\,I}$ absorbers are physically associated with galaxies whereas weak Ly$\alpha$ lines have no direct physical connection (Chen et al. 2005; Shone et al. 2010).

Turning to O VI absorption, Figure 5 shows the galaxy at the closest impact parameter to the 30 published O VI absorbers along our quasar sight lines with $0.02 < z < 0.2$ (Table 7). This includes five O VI systems where we have not identified a galaxy within 1 Mpc of the sight line with $|\delta v| < 400\,\mathrm{km\,s^{-1}}$. The rate of non-detections is much lower[14] than that observed for weak Ly$\alpha$ lines. Of course, only a few of the O VI systems have low H I column densities ($N_{\rm H\,I} < 10^{14}\,\mathrm{cm^{-2}}$). Ignoring the non-detections, the median impact parameter to a galaxy is approximately 200 kpc (consistent with the results of Stocke et al. 2006). This offset is smaller than that observed for Ly$\alpha$ lines having $N_{\rm H\,I} \approx 10^{14}\,\mathrm{cm^{-2}}$. On the other hand, only a small fraction of the O VI systems (5/30) have a galaxy detected within 100 kpc and only 1/18 for $N_{\rm O\,VI} < 10^{14}\,\mathrm{cm^{-2}}$. There are very few cases in the sample where one would insist that the sight line has intersected the virialized halo of the associated galaxy. Instead, the O VI gas appears linked to the extended CGM of galaxies on scales of a few hundred kpc. The luminosities of the nearest neighbors include galaxies at a wide range of luminosity and spectral type, with a preference toward late-type sub-$L^*$ systems. There is an apparent trend of decreasing $\rho$ with increasing $N_{\rm O\,VI}$ for the range of values considered in our analysis, but this is tempered by the large scatter in these quantities.

As emphasized at the start of this sub-section, the results presented in Figures 4 and 5 are subject to the incompleteness of our galaxy survey. In particular, one may argue that a population of fainter galaxies lies at smaller impact parameters than the sample comprising our survey. This could significantly affect our inferences regarding the roles of virialized halos and the extended CGM in hosting Ly$\alpha$/O VI absorption. To assess this concern, Table 7 lists the luminosity limit for each absorber and the completeness of the galaxy survey to that limit for $\rho = 150$ kpc. Regarding completeness, with the exception of two fields (PG1116+215 and PG1211+143), we obtained a redshift for every galaxy within $\rho = 150$ kpc of the O VI absorber to the magnitude limit $R = 19.5$ mag. We are confident, therefore, that no galaxy of comparable luminosity lies at closer distance to the sight line than the ones we have discovered.[15] Regarding the luminosity limit, a subset of the galaxies lie within twice the limit yet ≈40% are 5× brighter than the formal limit. Furthermore, owing to the details of mask design and specific scientific interests, we have surveyed several fields to $R > 19.5$ mag albeit with lower completeness. The galaxies discovered to these fainter magnitudes have been included in the analysis. We conclude, therefore, that our results

[14] This lends further support to the assertion that the lower fraction of weak H I absorbers associated with galaxies is not driven by incompleteness in the LCO/WFCCD galaxy survey.

[15] Although we are not sensitive to galaxies at very small impact parameters to the quasar (i.e., $\theta \lesssim 1''$ or $\rho \lesssim 20$ kpc for the redshifts considered), we expect these to be very rare occurrences and note that none of the sight lines exhibit very large H I column densities ($N_{\rm H\,I} \gg 10^{17}\,\mathrm{cm^{-2}}$).

**Table 7**
O VI Absorbers Identified in our Fields

| Field | $z_{\rm O\,VI}$ | $W^{\rm O\,VI}$ (mÅ) | $N_{\rm O\,VI}$ | Ref | $z_{\rm n}$[a] | $\rho_{\rm n}$[a] (kpc) | $L_{\rm n}$[a] ($L^*$) | $L_{\rm lim}$[b] ($L^*$) | $C$[c] |
|---|---|---|---|---|---|---|---|---|---|
| | | | | $0.005 < z < 0.02$ | | | | | |
| PG1116+215 | 0.0050 | ... | 13.91 | 4 | ... | ... | ... | 0.000 | 66 |
| PG1211+143 | 0.0071 | ... | 13.78 | 3 | ... | ... | ... | 0.001 | 52 |
| 3C273 | 0.0033 | 31 | 13.41 | 1 | ... | ... | ... | 0.000 | 73 |
| 3C273 | 0.0076 | 14 | 13.11 | 3 | ... | ... | ... | 0.001 | 74 |
| FJ2155−0922 | 0.0173 | <350 | 13.90 | 4 | ... | ... | ... | 0.003 | 100 |
| | | | | $0.02 < z < 0.2$ | | | | | |
| TONS180 | 0.0456 | 62 | 13.74 | 4 | 0.0456 | 277 | 0.397 | 0.022 | 100 |
| TONS180 | 0.0234 | 43 | 13.48 | 4 | 0.0234 | 154 | 0.021 | 0.006 | 100 |
| TONS180 | 0.0436 | 31 | 13.43 | 4 | ... | ... | ... | 0.020 | 100 |
| PKS0312−77 | 0.1983 | 64 | 13.84 | 1 | 0.1982 | 713 | 0.862 | 0.509 | 100 |
| PKS0312−77 | 0.1589 | 86 | 13.94 | 1 | ... | ... | ... | 0.311 | 100 |
| PKS0405−123 | 0.0918 | 49 | 13.58 | 4 | 0.0906 | 428 | 0.074 | 0.095 | 100 |
| PKS0405−123 | 0.0966 | 59 | 13.71 | 3 | 0.0965 | 267 | 0.164 | 0.106 | 100 |
| PKS0405−123 | 0.1669 | 412 | 14.64 | 1 | 0.1670 | 98 | 0.088 | 0.347 | 100 |
| PKS0405−123 | 0.1829 | 84 | 13.94 | 1 | ... | ... | ... | 0.425 | 100 |
| PG1116+215 | 0.1655 | 111 | 14.08 | 1 | 0.1660 | 163 | 0.369 | 0.341 | 75 |
| PG1116+215 | 0.1385 | 83 | 13.95 | 1 | 0.1383 | 136 | 2.231 | 0.230 | 80 |
| PG1116+215 | 0.0593 | 63 | 13.77 | 1 | 0.0600 | 130 | 0.113 | 0.038 | 67 |
| PG1211+143 | 0.0513 | ... | 14.30 | 4 | 0.0511 | 136 | 0.902 | 0.028 | 70 |
| PG1211+143 | 0.0645 | 144 | 14.16 | 3 | 0.0646 | 72 | 0.092 | 0.045 | 75 |
| PG1216+069 | 0.1236 | 378 | 14.70 | 1 | 0.1241 | 92 | 0.711 | 0.180 | 100 |
| 3C273 | 0.0902 | 16 | 13.13 | 1 | 0.0902 | 463 | 1.206 | 0.091 | 100 |
| 3C273 | 0.1200 | 24 | 13.33 | 1 | ... | ... | ... | 0.169 | 100 |
| PKS1302−102 | 0.0940 | 19 | 13.15 | 4 | 0.0936 | 67 | 0.213 | 0.100 | 100 |
| PKS1302−102 | 0.0647 | 69 | 13.70 | 3 | 0.0647 | 353 | 0.054 | 0.045 | 100 |
| PKS1302−102 | 0.0989 | ... | 14.03 | 3 | ... | ... | ... | 0.111 | 100 |
| PKS1302−102 | 0.0423 | 194 | 14.38 | 3 | 0.0426 | 221 | 2.804 | 0.019 | 80 |
| PKS1302−102 | 0.1453 | 146 | 14.16 | 4 | 0.1453 | 87 | 0.433 | 0.256 | 100 |
| PKS1302−102 | 0.1916 | 80 | 13.93 | 1 | 0.1917 | 219 | 0.974 | 0.471 | 100 |
| MRK1383 | 0.0519 | 66 | 13.83 | 4 | ... | ... | ... | 0.029 | 75 |
| FJ2155−0922 | 0.1579 | 120 | 14.08 | 1 | 0.1581 | 352 | 0.543 | 0.307 | 100 |
| FJ2155−0922 | 0.1324 | 225 | 14.39 | 1 | 0.1326 | 222 | 1.779 | 0.209 | 100 |
| FJ2155−0922 | 0.0776 | 46 | 13.61 | 1 | 0.0788 | 232 | 0.172 | 0.066 | 100 |
| FJ2155−0922 | 0.1765 | ... | 14.44 | 1 | 0.1764 | 347 | 2.631 | 0.393 | 100 |
| PKS2155−304 | 0.0571 | 44 | 13.57 | 3 | 0.0570 | 424 | 1.736 | 0.035 | 100 |
| PKS2155−304 | 0.0541 | 32 | 13.63 | 3 | 0.0541 | 567 | 2.235 | 0.031 | 100 |
| | | | | $z > 0.2$ | | | | | |
| PKS0312−77 | 0.2027 | 538 | 14.91 | 1 | 0.2026 | 133 | 0.696 | 0.535 | 100 |
| PKS0405−123 | 0.4950 | 213 | 14.44 | 1 | ... | ... | ... | 4.303 | 100 |
| PKS0405−123 | 0.3509 | 24 | 13.35 | 3 | 0.3520 | 165 | 0.302 | 1.891 | 100 |
| PKS0405−123 | 0.3616 | 96 | 14.00 | 1 | 0.3612 | 225 | 7.318 | 2.029 | 100 |
| PKS0405−123 | 0.3634 | 38 | 13.61 | 1 | ... | ... | ... | 2.053 | 100 |
| PG1216+069 | 0.2677 | 22 | 13.30 | 1 | ... | ... | ... | 1.007 | 100 |
| PG1216+069 | 0.2819 | 94 | 13.95 | 1 | ... | ... | ... | 1.134 | 100 |
| PKS1302−102 | 0.2274 | 40 | 13.59 | 1 | ... | ... | ... | 0.694 | 100 |
| PKS1302−102 | 0.2256 | 82 | 13.93 | 1 | 0.2256 | 437 | 0.981 | 0.681 | 100 |
| PKS1302−102 | 0.2044 | 33 | 13.64 | 3 | ... | ... | ... | 0.545 | 100 |
| PKS1302−102 | 0.2529 | 11 | 12.92 | 3 | ... | ... | ... | 0.883 | 100 |

**Notes.** The analysis presented in Section 3.2 only considers O VI systems with $0.02 < z < 0.2$ to minimize incompleteness in the galaxy survey.
[a] Redshift, impact parameter, and luminosity of the brightest galaxy ($L > 0.1\,L^*$) within 200 kpc and $|\delta v| < 400\,{\rm km\,s^{-1}}$ (if any).
[b] Limiting luminosity of the galaxy survey at the redshift of the absorber.
[c] Completeness of the galaxy survey to $R = 19.5$ mag within the radius corresponding to $\rho = 150$ kpc at the O VI absorber's redshift.
**References.** (1) Tripp et al. 2008; (3) Danforth & Shull 2008; (4) Danforth et al. 2006.

are unlikely to be severely compromised by a lack of sensitivity to fainter galaxies.

Another (brute force) approach to assess the effects of incompleteness is to obtain significantly deeper spectroscopy in the fields. Chen & Mulchaey (2009) have performed a galaxy survey with the IMACS and LDSS3 spectrometers on the 6.5 m Magellan telescopes for two of our fields (PKS0405–123 and PG1216+069). They achieved a high completeness around each quasar sight line to several magnitudes fainter limits (≈10× deeper). For the PKS0405–123 field, they do identify a new dwarf galaxy associated with the $z = 0.0918$ O VI absorber which lies at closer impact parameter ($\rho = 73$ kpc) than the

dwarf galaxy we had discussed. This is, however, the only modification for the four O VI absorbers within the redshift interval $0.02 < z < 0.2$, and even this galaxy is at an impact parameter that may exceed its virialized halo. For the PG1216+069 field, Chen & Mulchaey (2009) find no fainter galaxies at closer impact parameters for the $z = 0.125$ sub-$L^*$ galaxy identified in our survey. Similar results were derived from a deep Gemini/GMOS analysis of the field surrounding PG0953+414 (Tripp et al. 2006b).

## 4. DISCUSSION

The previous section described the association of Ly$\alpha$ and O VI absorption with galaxies discovered in our LCO/WFCCD survey (Paper IV). In Section 3.1, we explored the strength of Ly$\alpha$ and O VI absorption as a function of galaxy luminosity, spectral type, and impact parameter. We then reported on the results of a search for galaxies related to Ly$\alpha$ and O VI absorption (Section 3.2). In this section, we synthesize these results and discuss the implications in the context of previous observational and theoretical work. We divide the discussion by transition (i.e., Ly$\alpha$ and O VI) but emphasize that a complete description of the IGM must consider both elements.

### 4.1. Ly$\alpha$

The Ly$\alpha$ transition is the strongest and most commonly observed transition of the IGM. Its complex pattern of absorption defines the so-called Ly$\alpha$ forest and sets the starting point for nearly all IGM analysis. The current cosmological paradigm for the Ly$\alpha$ forest is that these lines arise from an undulating Gunn–Peterson field of overdensities (e.g., Miralda-Escudé et al. 1996). In turn, observations of the IGM provide direct constraints for cosmological parameters (e.g., Dunkley et al. 2009). This gas is also predicted to be the dominant baryonic reservoir of the universe, which fuels the formation and growth of galaxies.

We begin with a discussion of the properties of H I gas surrounding low-$z$ galaxies ($\rho < 300$ kpc). Several previous studies have examined the incidence of Ly$\alpha$ absorption for galaxies located at small impact parameters to quasar sight lines. In each case, the authors have reported a very high detection rate for galaxies within a few hundred kpc: Chen et al. (2001a) found positive detections for 29/31 of their predominantly $L^*$ galaxies to $\rho = 250\,h_{72}^{-1}$ kpc with $W^{\rm Ly\alpha} > 300$ mÅ and reported a sharp decline at larger impact parameter, Bowen et al. (2002) detected Ly$\alpha$ lines with $N_{\rm H\,I} \geqslant 10^{13}$ cm$^{-2}$ for 8/8 of the galaxies located within $\rho = 280\,h_{72}^{-1}$ kpc of their quasar sight lines, and Wakker & Savage (2009) reported positive detections for 7/7 of the $L \geqslant 0.1\,L^*$ field galaxies in their sample when restricting to $\rho \leqslant 350$ kpc.

With our LCO/WFCCD survey we have examined a sample of 37 galaxies at $\rho < 300$ kpc with greater emphasis on lower luminosities than previous work. The results presented in Figures 1–3 (Tables 3–5) further solidify the correlation between galaxies and Ly$\alpha$ absorption: to an impact parameter of $\rho \approx 300$ kpc, we observe a nearly 100% probability for detecting Ly$\alpha$ absorption ($W^{\rm Ly\alpha} > 50$ mÅ) within 400 km s$^{-1}$ of a galaxy. This result is independent of galaxy luminosity (for $L > 0.01\,L^*$), spectral type, and local environment[16] (defined by the number of close neighbors). Altogether, these results demand that low-$z$ galaxies of all types are embedded within a diffuse, highly ionized medium with a very high covering fraction to significant H I absorption. We refer to this medium as the CGM, although this gas need not be physically associated (e.g., bound) with the galaxy.

Before considering the origin of this medium, we review and then explore its physical properties. First, we note that the Doppler parameters that are typical of low-$z$ Ly$\alpha$ lines generally require kinetic temperatures $T < 10^5$ K (e.g., Davé et al. 1999; Williger et al. 2006). The standard expectation is that the majority of these absorbers trace photoionized gas with $T \sim 10^4$ K. For those absorption systems that also exhibit metal-line transitions (e.g., C IV, C III, O VI), this hypothesis may be tested against ionization modeling and the results are usually consistent with a photoionized medium (e.g., Prochaska et al. 2004; Cooksey et al. 2008). This modeling also provides a constraint on the ionization fraction and an estimate of the total hydrogen column density $N_{\rm H}$.

A remarkable result for the low-$z$ IGM is that the estimated $N_{\rm H}$ values are uniform at $\approx 10^{19}$ cm$^{-2}$, i.e., independent of the observed $N_{\rm H\,I}$ value (Prochaska et al. 2004; Lehner et al. 2007). This "$N_{\rm H}$ constancy" was interpreted by Prochaska et al. (2004) to result from lower $N_{\rm H\,I}$ absorbers having lower average volume density (e.g., Davé et al. 1999) which implies a higher ionization correction for a uniform (background) radiation field. Indeed, analyses of recent simulations of the low-$z$ IGM have considered the $N_{\rm H}$ constancy explicitly and have reproduced the observed result with a similar explanation (Davé et al. 2010). We caution that this $N_{\rm H}$ constancy was derived empirically from absorbers with $N_{\rm H\,I} \approx 10^{13.5}$–$10^{15}$ cm$^{-2}$ which had no known association with galaxies. We demonstrate below, however, that the majority of the stronger $N_{\rm H\,I}$ systems must be associated with galaxies.

Adopting a constant $N_{\rm H}$ value for the observed Ly$\alpha$ forest, we may crudely estimate the mass of the photoionized CGM surrounding low-$z$ galaxies. A simple estimate follows from the characteristic hydrogen column density $N_{\rm H,CGM}$ and a characteristic radius $r_{\rm CGM}$:

$$M_{\rm CGM} = N_{\rm H,CGM} m_p \mu \pi r_{\rm CGM}^2, \quad (2)$$

with the factor $\mu \approx 1.3$ accounting for helium. For our assumed values, we find

$$M_{\rm CGM} \approx 3 \times 10^{10}\,M_\odot \left(\frac{N_{\rm H,CGM}}{10^{19}\,{\rm cm}^{-2}}\right)\left(\frac{r_{\rm CGM}}{300\,{\rm kpc}}\right)^2. \quad (3)$$

Therefore, we estimate a baryonic reservoir surrounding each galaxy which meets or significantly exceeds the typical baryonic mass of present-day sub-$L^*$ galaxies. Again, this CGM need not be physically associated (e.g., gravitationally bound) with the galaxy. Nevertheless, it represents a large baryonic reservoir for future star formation or could even (in part) be gas that was expelled during the processes of galaxy formation. Indeed, adopting this mass for all galaxies with $L > 0.01\,L^*$, one estimates a mass density $\rho_{\rm CGM} \sim M_{\rm CGM}\, n_{L>0.1L^*}$ that is approximately 10% of the total baryonic mass density, $\Omega_{\rm CGM} \approx 0.1\Omega_{\rm b}$. Lastly, if the gas is metal enriched, the mass in metals could exceed the amount metals locked in stars within these galaxies.

[16] Our results do not confirm the findings of Wakker & Savage (2009) that galaxies in groups exhibit systematically weaker Ly$\alpha$ absorption, although we have not yet constructed a well-defined group sample from the LCO/WFCCD survey.

**Table 8**
Galaxies within 1 Mpc of a QSO Sight Line

| Field | R.A. (J2000) | Decl. (J2000) | $z_{gal}$ | $\rho$ (kpc) | $L$ ($L_*$) | $z_{abs}^{Ly\alpha}$ | $W^{Ly\alpha}$ (mÅ) | $N_{H\,I}$ | Ref. | $z_{abs}^{O\,VI}$ | $W^{O\,VI}$ (mÅ) | $N_{O\,VI}$ | Ref |
|---|---|---|---|---|---|---|---|---|---|---|---|---|---|
| Q0026+1259 | 00:29:09.32 | +13:16:28.5 | 0.0329 | 45 | 0.019 | ... | ... | ... | ... | 0.0329 | <120 | <14.00 | 9 |
| | 00:29:15.36 | +13:20:57.0 | 0.0393 | 222 | 1.505 | ... | ... | ... | ... | 0.0393 | <120 | <14.00 | 9 |
| | 00:28:53.55 | +13:24:19.9 | 0.0565 | 620 | 0.608 | ... | ... | ... | ... | ... | ... | ... | ... |
| | 00:29:53.44 | +13:10:49.5 | 0.0738 | 919 | 0.203 | ... | ... | ... | ... | ... | ... | ... | ... |
| | 00:29:16.48 | +13:21:52.9 | 0.0804 | 519 | 0.123 | ... | ... | ... | ... | ... | ... | ... | ... |
| | 00:29:37.55 | +13:10:21.0 | 0.0961 | 858 | 2.137 | ... | ... | ... | ... | 0.0961 | <100 | <14.00 | 9 |
| | 00:29:23.49 | +13:09:40.8 | 0.1125 | 817 | 1.192 | ... | ... | ... | ... | 0.1125 | <100 | <14.00 | 9 |
| | 00:29:16.04 | +13:10:02.5 | 0.1314 | 828 | 0.195 | ... | ... | ... | ... | ... | ... | ... | ... |
| TONS180 | 00:57:04.01 | −22:26:51.2 | 0.0234 | 154 | 0.021 | 0.0234 | 222 | 13.80 | 5 | 0.0234 | 43 | 13.48 | 4 |
| | 00:57:08.52 | −22:18:29.6 | 0.0456 | 276 | 0.397 | 0.0456 | 212 | 13.80 | 5 | 0.0456 | 62 | 13.74 | 4 |

**Notes.** Galaxies within $\pm 400\,km\,s^{-1}$ in redshift were grouped together and only the member with smallest impact parameter is tabulated here.

(This table is available in its entirety in a machine-readable form in the online journal. A portion is shown here for guidance regarding its form and content.)

The near unity covering fraction of this CGM for Ly$\alpha$ absorption to $\rho \approx 300$ kpc inspires us to examine further its radial extent. Previously, Chen et al. (2001b) reported a decline in the average Ly$\alpha$ equivalent width for $\rho \gtrsim 250$ kpc. Similarly, Tripp et al. (1998) and Wakker & Savage (2009) noted a lower detection rate and average Ly$\alpha$ equivalent width for $L \approx L^*$ galaxies to $\rho \gtrsim 1$ Mpc. In Figure 6 (Table 8), we have extended the analysis of our LCO/WFCCD survey to $\rho = 1$ Mpc. Here, we include galaxies of all luminosity and plot only the closest galaxy to the sight line without repeating any pair of galaxies with $|\delta v| < 400\,km\,s^{-1}$. We also include the galaxy survey in the field of PKS0405–123 performed by Williger et al. (2006). There are two issues to emphasize before proceeding: (1) incompleteness in our galaxy survey implies that the $\rho$ values are strictly upper limits, i.e., another (probably fainter) galaxy may exist at smaller impact parameter, and (2) there may be little physical connection (e.g., gravitational interaction) between this gas and the galaxy on such large scales. Nevertheless, the results may offer a valuable constraint for galaxy/IGM models and provide further insight into the galaxy/absorber connection.

There are two obvious conclusions to draw from Figure 6: (1) the median equivalent width decreases with increasing $\rho$ and (2) the detection rate declines beyond $\rho \approx 300$ kpc but apparently remains above the random rate (≈10%; Section 3.1) out to at least 1 Mpc. These conclusions are not independent, e.g., the median $W^{Ly\alpha}$ value is significantly lower at $\rho > 500$ kpc because of the lower detection rate. A Spearman's correlation test of only the *detections* reports that the null hypothesis of no correlation is ruled out at >99.99% c.l. This anti-correlation is only strengthened by the non-detections, and it is not a natural consequence of incompleteness in the galaxy survey. We have performed a simple linear regression on the positive detections in log–log space, i.e., by assuming $W^{Ly\alpha}(\rho) = W_0(\rho/1\,kpc)^{-\gamma}$. If we ignore the $L^*$ galaxies (for reasons discussed below) and perform a linear regression on the remaining galaxies with detections, we recover $W_0 = 4.0$ Å and $\gamma = -0.69$. These values are in good agreement with Tripp et al. (1998), whose analysis was performed on a heterogenous set of galaxy samples. We also note that the $W^{Ly\alpha}$ values have a shallower trend with impact parameter for $\rho > 100$ kpc. Removing those galaxy/absorber pairs from the linear regression, we recover $W_0 = 3.3$ Å and $\gamma = -0.43$. These values may better describe evolution in the large-scale structures that surround low-$z$ galaxies. We also stress that a rank-correlation test on the

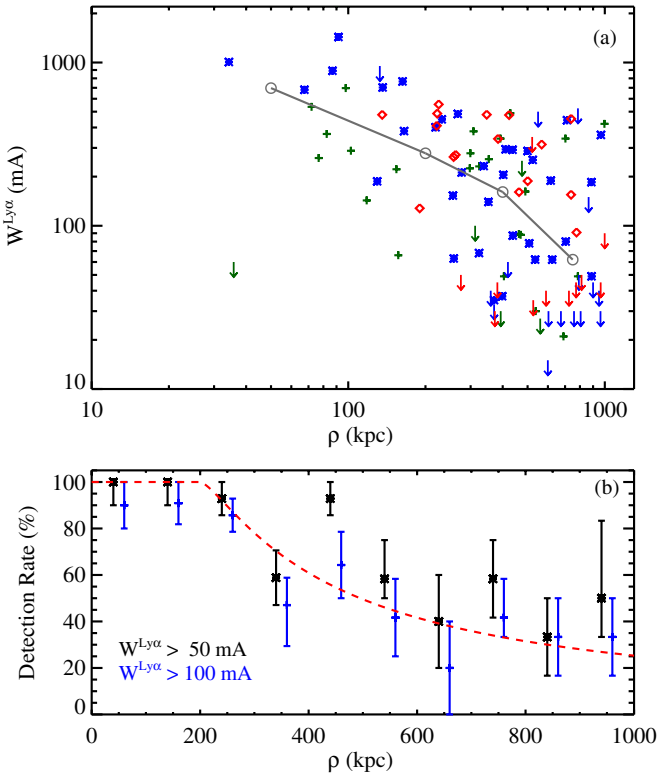


**Figure 6.** (a) Measurements of associated Ly$\alpha$ absorption for galaxies of all luminosity in our sample within 1 Mpc of a quasar sight line with UV spectral coverage of the Ly$\alpha$ line. We have grouped galaxies together in intervals of 400 km s$^{-1}$ and only plot the system nearest to the sight line. Red diamonds indicate $L^*$ galaxies, blue asterisks are sub-$L^*$ galaxies, and green plus signs indicate dwarf galaxies. Arrows of the same colors represent non-detections for galaxies of these luminosities. There is a strong anti-correlation between Ly$\alpha$ equivalent width (and column density) and impact parameter. Furthermore, there is a very high incidence of positive detections to 50 mÅ to $\rho \approx 500$ kpc and a marked decline at larger impact parameter. The gray circles and line trace the median equivalent width (including limits) in bins of $\rho$ = [0–100] kpc, [100–300] kpc, [300–500] kpc, [500–1000] kpc (Table 6). (b) Detection rate of an Ly$\alpha$ line within 400 km s$^{-1}$ of the galaxies in the LCO/WFCCD survey as a function of impact parameter, for two limiting equivalent widths. Error bars reflect a bootstrap analysis which provides a crude estimate of the uncertainty in the measurements. The dashed red line indicates the prediction for the detection rate for a simplistic filamentary model with filamentary width $w \approx 400$ kpc (see the text for details).

(A color version of this figure is available in the online journal.)

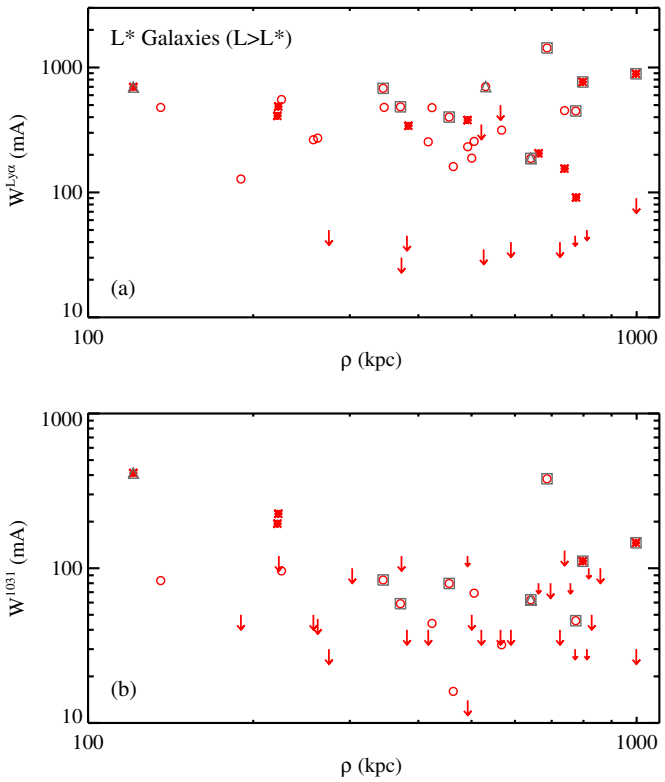


**Figure 7.** (a) Measured Ly$\alpha$ equivalent widths for every $L^*$ galaxy in the LCO/WFCCD survey (with the closest galaxy shown for cases with two or more within 400 km s$^{-1}$) as a function of impact parameter, extending to 1 Mpc. Galaxies with early-type spectra are marked with open circles and those with late-type spectra are plotted as asterisks. Small/large arrows denote limits for late/early-type spectra. The squares (triangles) indicate cases where an additional sub-$L^*$ (dwarf) galaxy with consistent redshift lies closer to the sight line. The galaxies exhibit two sets of $W^{Ly\alpha}$ measurements: (1) positive detections with $W^{Ly\alpha} > 200$ mÅ and (2) a population of non-detections with $W^{Ly\alpha} < 100$ mÅ (generally $< 50$ mÅ). (b) Equivalent width of O VI 1031 as a function of impact parameter for $L^*$ galaxies from the LCO/WFCCD survey. Symbols have the same meaning as in (a). Only a small fraction of these galaxies exhibit a positive O VI detection for $\rho > 250$ kpc, especially if one excludes the systems where a closer, fainter galaxy exists at the same redshift. These results indicate that $L^*$ galaxies are not surrounded by a CGM to many hundred kpc with a high covering fraction to significant O VI absorption.

(A color version of this figure is available in the online journal.)

detections and upper limits for galaxies at $\rho > 200$ kpc rules out the null hypothesis at >99.93% c.l. Both the detection rate and median equivalent width of Ly$\alpha$ absorption are correlated with galaxy impact parameter to at least 1 Mpc, i.e., far beyond the virialized halos and presumed CGM of these galaxies. Before concluding, we note that a power-law description for $W^{Ly\alpha}(\rho)$ was not physically motivated. Furthermore, despite the significant anti-correlation, it is not a very good description of the data; there is tremendous scatter about the regression at all impact parameters.

A closer inspection of Figure 6 reveals that the Ly$\alpha$ detections for $L^*$ galaxies do not follow the trend of decreasing $W^{Ly\alpha}$ with increasing $\rho$. In fact, the $W^{Ly\alpha}$ values for these galaxies form two sets: the galaxies with positive detections show $W^{Ly\alpha} > 100$ mÅ (generally $W^{Ly\alpha} > 200$ mÅ), yet approximately half of the $L^*$ galaxies have no associated absorption to very sensitive limits ($W^{Ly\alpha} < 50$ mÅ). This phenomenon is highlighted in Figure 7 where we plot $W^{Ly\alpha}$ versus $\rho$ for every $L^*$ galaxy within 1 Mpc, showing the closest galaxy to the sight line in cases where two or more $L^*$ galaxies lie within $\pm 400$ km s$^{-1}$ of one another (Table 9). Again, the positive detections primarily result in $W^{Ly\alpha} > 200$ mÅ and approximately half of the systems (without a fainter, neighboring galaxy with smaller $\rho$) have a non-detection with $W^{Ly\alpha} < 100$ mÅ. We find no clear differences in the Ly$\alpha$ detection rate or $W^{Ly\alpha}$ values for these galaxies as a function of spectral type or redshift. We hypothesize that the subset without a detection could be sight lines penetrating a hot (e.g., virialized) gas which has collisionally ionized hydrogen to non-detectable levels. The positive detections, in contrast, would arise from gas that has not been shock heated or has since cooled. This simple scenario, however, may not naturally explain the nearly constant $W^{Ly\alpha}$ values for the positive detections.

To summarize the discussion thus far, our results (and previous work) demonstrate that galaxies of all types are surrounded by a highly ionized medium (which we term as an extended CGM) with near unity covering fraction to Ly$\alpha$ absorption to $\rho \approx 300$ kpc. Furthermore, galaxies of all types exhibit a declining detection rate for H I absorption with $W^{Ly\alpha} > 50$ mÅ to $\rho \approx 1$ Mpc. A key question motivated by these results is what fraction of the Ly$\alpha$ forest arises from the CGM surrounding galaxies? More bluntly, can the virialized halos and extended CGM of galaxies account for the majority of lines in the observed Ly$\alpha$ forest? These questions frame the long-standing debate on whether Ly$\alpha$ absorbers arise primarily from the gaseous halos of galaxies or from the large-scale, overdense medium (e.g., filaments) that encompasses them. To a large degree, the argument hinges on whether the structures giving rise to Ly$\alpha$ absorption have dimensions of several hundred kpc or are greater than 1 Mpc.

It is evident from the results described above that a fraction of Ly$\alpha$ absorbers are closely associated with galaxies. Indeed, some fraction of the Ly$\alpha$ forest must arise from gas bound to individual galaxies. The majority of galaxy/absorber pairs in our sample, however, occur at impact parameters that significantly exceed the presumed virial radius of the galaxies. Indeed, the measured H I column densities are many orders of magnitude smaller than the surface densities characteristic of star-forming galaxies; the gas cannot be related to canonical H I disks nor even the tidal features regularly observed in 21 cm emission observations (e.g., Hibbard et al. 2001). We conclude, therefore, that Ly$\alpha$ absorption is generally unrelated to the inner galaxy and/or the processes of galaxy formation (e.g., winds, tidal stripping). Instead, the material we have associated with galaxies lies within their extended CGM. In this case the association need not be causal; the gas may not be bound to the galaxy and the two phenomena—galaxies and H I absorbers—may simply trace the same overdensities in the universe.

We draw further insight into the origin of the Ly$\alpha$ forest from the results presented in Figure 4. As has been emphasized previously (Penton et al. 2002; Chen et al. 2005; Morris & Jannuzi 2006), the origin of Ly$\alpha$ absorbers appears to be sensitive to the H I column density. At low $N_{\rm H\,I}$ values, the fraction of "random" absorbers that may be associated with a galaxy with $\rho < 300$ kpc is small (<20% [12/76] for $N_{\rm H\,I} = 10^{13}$–$10^{14}$ cm$^{-2}$). This suggests that the majority of weak Ly$\alpha$ absorbers, which dominate the Ly$\alpha$ forest by number, arise beyond the virialized halos and the CGM of individual galaxies. Presumably, these absorbers arise in overdense regions of the low-$z$ universe which have not supported the formation of a luminous galaxy. In contrast, the percentage of strong absorbers ($N_{\rm H\,I} > 10^{15}$ cm$^{-2}$) with an associated galaxy at $\rho < 300$ kpc is 80% (8/10). One is compelled, for this subset, to physically associate the absorbers with the galaxies. These inferences are supported by the $N_{\rm H\,I}$ dependence measured for the clustering of

**Table 9**
$L > L^*$ Galaxies within 1 Mpc of a QSO Sight Line

| Field | R.A. (J2000) | Decl. (J2000) | $z_{gal}$ | Type[a] | $\rho$ (kpc) | $L$ ($L^*$) | $\mathcal{N}$[b] | $z_{abs}^{Ly\alpha}$ | $W^{Ly\alpha}$ (mÅ) | $N_{H\,I}$ | Ref. | $z_{abs}^{O\,VI}$ | $W^{O\,VI}$ (mÅ) | $N_{O\,VI}$ | Ref. |
|---|---|---|---|---|---|---|---|---|---|---|---|---|---|---|---|
| Q0026+1259 | 00:29:15.36 | +13:20:57.0 | 0.0393 | Early | 222 | 1.505 | 0 | ... | ... | ... | ... | 0.0393 | <120 | <14.00 | 9 |
| | 00:29:37.55 | +13:10:21.0 | 0.0961 | Early | 858 | 2.137 | 0 | ... | ... | ... | ... | 0.0961 | <100 | <14.00 | 9 |
| | 00:29:23.49 | +13:09:40.8 | 0.1125 | Late | 817 | 1.192 | 0 | ... | ... | ... | ... | 0.1125 | <100 | <14.00 | 9 |
| PKS0312−77 | 03:12:31.11 | −76:43:25.0 | 0.0514 | Early | 722 | 5.338 | 4 | ... | ... | ... | ... | ... | ... | ... | ... |
| | 03:11:02.46 | −77:00:05.2 | 0.0529 | Early | 936 | 1.608 | 4 | ... | ... | ... | ... | ... | ... | ... | ... |
| | 03:11:58.58 | −76:48:55.4 | 0.1192 | Late | 383 | 2.018 | 1 | 0.1183 | 341 | 14.17 | 3 | ... | ... | ... | ... |
| PKS0405−123 | 04:08:06.63 | −12:12:50.9 | 0.0800 | Early | 416 | 1.531 | 4 | 0.0814 | 254 | 13.76 | 3 | 0.0800 | <40 | <13.50 | 9 |
| | 04:07:54.22 | −12:14:50.7 | 0.0967 | Early | 371 | 1.481 | 9 | 0.0966 | 484 | 14.64 | 3 | 0.0966 | 59 | 13.71 | 3 |
| | 04:07:44.03 | −12:12:09.5 | 0.1532 | Early | 189 | 1.073 | 1 | 0.1522 | 128 | 13.46 | 3 | 0.1522 | <50 | <13.60 | 9 |
| | 04:07:57.44 | −12:07:41.3 | 0.1617 | Late | 738 | 1.090 | 1 | 0.1612 | 155 | 13.62 | 3 | ... | ... | ... | ... |
| | 04:07:51.28 | −12:11:38.3 | 0.1670 | Late | 120 | 2.349 | 1 | 0.1671 | 697 | 15.47 | 3 | 0.1669 | 412 | 14.64 | 1 |
| | 04:07:42.79 | −12:11:33.1 | 0.2030 | Early | 274 | 1.175 | 9 | 0.2030 | <50 | <13.00 | 9 | 0.2030 | <30 | <13.40 | 9 |
| | 04:08:01.90 | −12:11:40.1 | 0.2484 | Late | 772 | 1.419 | 1 | 0.2484 | <45 | <12.90 | 9 | 0.2484 | <30 | <13.40 | 9 |
| | 04:07:34.68 | −12:13:22.6 | 0.2951 | Early | 998 | 1.322 | 3 | 0.2951 | <90 | <13.20 | 9 | 0.2951 | <30 | <13.40 | 9 |
| | 04:07:50.69 | −12:12:25.2 | 0.2976 | Early | 257 | 2.074 | 7 | 0.2977 | 264 | 13.85 | 3 | 0.2976 | <50 | <13.60 | 9 |
| | 04:07:52.33 | −12:14:08.0 | 0.3099 | Early | 724 | 1.979 | 3 | 0.3099 | <40 | <12.90 | 9 | 0.3099 | <40 | <13.50 | 9 |
| | 04:07:57.96 | −12:09:52.5 | 0.3203 | Late | 811 | 1.148 | 1 | 0.3203 | <50 | <13.00 | 9 | 0.3203 | <30 | <13.40 | 9 |
| | 04:07:50.24 | −12:09:52.2 | 0.3252 | Early | 500 | 2.562 | 0 | 0.3250 | 188 | 13.81 | 3 | 0.3252 | <50 | <13.60 | 9 |
| | 04:07:45.96 | −12:11:09.9 | 0.3612 | Early | 225 | 7.318 | 5 | 0.3608 | 554 | 15.14 | 3 | 0.3616 | 96 | 14.00 | 1 |
| | 04:07:51.88 | −12:13:16.6 | 0.4253 | Early | 617 | 6.851 | 5 | ... | ... | ... | ... | ... | ... | ... | ... |
| | 04:07:55.50 | −12:10:37.0 | 0.4282 | Unkn | 673 | 1.208 | 2 | ... | ... | ... | ... | ... | ... | ... | ... |
| | 04:07:41.00 | −12:13:15.4 | 0.5563 | Unkn | 944 | 2.075 | 0 | ... | ... | ... | ... | ... | ... | ... | ... |
| PG1004+130 | 10:07:34.55 | +12:52:09.5 | 0.0704 | Early | 303 | 2.619 | 0 | ... | ... | ... | ... | 0.0704 | <100 | <13.90 | 9 |
| | 10:07:25.39 | +12:53:04.8 | 0.1674 | Early | 696 | 3.920 | 2 | ... | ... | ... | ... | 0.1674 | <80 | <13.80 | 9 |
| | 10:07:10.67 | +12:50:04.3 | 0.1931 | Late | 757 | 1.469 | 3 | ... | ... | ... | ... | 0.1931 | <80 | <13.80 | 9 |
| PG1116+215 | 11:19:24.31 | +21:10:30.6 | 0.0590 | Early | 641 | 1.545 | 3 | 0.0593 | 187 | 13.64 | 1 | 0.0593 | 63 | 13.77 | 1 |
| | 11:19:06.73 | +21:18:29.3 | 0.1383 | Early | 135 | 2.231 | 4 | 0.1385 | 479 | >14.35 | 1 | 0.1385 | 83 | 13.95 | 1 |
| | 11:19:16.88 | +21:14:57.1 | 0.1652 | Late | 797 | 1.260 | 14 | 0.1655 | 765 | >14.43 | 1 | 0.1655 | 111 | 14.08 | 1 |
| PG1211+143 | 12:14:01.15 | +14:11:07.2 | 0.0522 | Early | 530 | 1.318 | 6 | 0.0510 | 703 | 15.67 | 3 | 0.0513 | ... | 14.30 | 4 |
| PG1216+069 | 12:19:30.89 | +06:43:34.6 | 0.0805 | Late | 491 | 2.456 | 2 | 0.0805 | 379 | 13.87 | 3 | 0.0815 | <120 | <14.00 | 9 |
| | 12:19:33.88 | +06:42:44.2 | 0.1250 | Early | 686 | 1.955 | 4 | 0.1236 | 1433 | >14.78 | 1 | 0.1236 | 378 | 14.70 | 1 |
| | 12:19:40.27 | +06:40:41.2 | 0.1354 | Early | 738 | 2.421 | 4 | 0.1350 | 452 | 15.12 | 3 | 0.1354 | <130 | <14.10 | 9 |
| | 12:19:06.47 | +06:39:28.8 | 0.1810 | Late | 662 | 2.622 | 3 | 0.1808 | 205 | 14.38 | 3 | 0.1810 | <80 | <13.80 | 9 |
| | 12:19:04.05 | +06:41:35.6 | 0.1917 | Unkn | 963 | 1.255 | 3 | 0.1917 | <45 | <12.90 | 9 | 0.1917 | <40 | <13.50 | 9 |
| | 12:19:20.39 | +06:36:57.6 | 0.2464 | Early | 381 | 1.934 | 0 | 0.2464 | <45 | <12.90 | 9 | 0.2464 | <40 | <13.50 | 9 |
| 3C273 | 12:28:51.89 | +02:06:03.2 | 0.0902 | Early | 463 | 1.206 | 0 | 0.0902 | 161 | 13.53 | 1 | 0.0902 | 16 | 13.13 | 1 |
| PKS1302−102 | 13:05:20.22 | −10:36:30.4 | 0.0426 | Late | 221 | 2.804 | 1 | 0.0422 | 410 | 14.83 | 3 | 0.0422 | 194 | 14.38 | 3 |
| | 13:05:14.84 | −10:40:00.4 | 0.0569 | Early | 521 | 1.217 | 0 | 0.0569 | <350 | <15.00 | 9 | 0.0569 | <40 | <13.50 | 9 |
| | 13:05:41.01 | −10:26:42.5 | 0.0652 | Early | 505 | 2.120 | 0 | 0.0647 | 256 | 14.06 | 3 | 0.0647 | 69 | 13.70 | 3 |
| | 13:05:30.32 | −10:26:17.2 | 0.0718 | Early | 564 | 2.615 | 1 | 0.0712 | <500 | <16.00 | 9 | 0.0718 | <40 | <13.50 | 9 |
| | 13:05:20.96 | −10:34:51.5 | 0.0939 | Early | 345 | 5.872 | 9 | 0.0949 | 681 | 15.35 | 3 | 0.0948 | 84 | 13.75 | 4 |
| | 13:05:30.68 | −10:36:55.6 | 0.1393 | Early | 526 | 1.029 | 5 | 0.1393 | <35 | <12.80 | 9 | ... | ... | ... | ... |
| | 13:05:40.17 | −10:36:54.2 | 0.1429 | Early | 589 | 2.245 | 1 | 0.1429 | <40 | <12.90 | 9 | 0.1429 | <40 | <13.50 | 9 |
| | 13:05:34.00 | −10:39:59.6 | 0.1454 | Late | 997 | 1.172 | 3 | 0.1453 | 890 | 15.29 | 3 | 0.1453 | 146 | 14.16 | 4 |
| | 13:05:31.29 | −10:35:42.1 | 0.1924 | Early | 455 | 1.682 | 3 | 0.1916 | 401 | 15.01 | 3 | 0.1916 | 80 | 13.93 | 1 |
| FJ2155−0922 | 21:54:56.64 | −09:18:07.9 | 0.0517 | Early | 262 | 1.553 | 0 | 0.0515 | 272 | 14.08 | 3 | 0.0514 | <47 | <13.62 | 4 |
| | 21:55:22.71 | −09:23:51.8 | 0.0600 | Early | 372 | 1.900 | 6 | 0.0600 | <30 | <12.70 | 9 | 0.0600 | <120 | <14.00 | 9 |
| | 21:55:17.31 | −09:17:51.8 | 0.0734 | Early | 492 | 4.072 | 3 | 0.0736 | 232 | 14.64 | 3 | 0.0734 | <14 | <13.06 | 4 |
| | 21:54:34.63 | −09:16:32.6 | 0.0785 | Early | 774 | 1.716 | 21 | 0.0777 | 448 | >14.29 | 1 | 0.0777 | 46 | 13.61 | 1 |
| | 21:55:00.63 | −09:31:28.6 | 0.0831 | Early | 828 | 3.249 | 1 | ... | ... | ... | ... | 0.0831 | <50 | <13.60 | 9 |
| | 21:55:06.53 | −09:23:25.2 | 0.1326 | Late | 222 | 1.779 | 2 | 0.1324 | 487 | >14.30 | 1 | 0.1324 | 225 | 14.39 | 1 |
| | 21:54:54.91 | −09:23:30.8 | 0.1764 | Early | 346 | 2.631 | 0 | 0.1765 | 479 | >14.27 | 1 | 0.1765 | ... | 14.44 | 1 |
| | 21:55:18.64 | −09:23:02.7 | 0.1813 | Late | 775 | 1.065 | 0 | 0.1808 | 91 | <0.00 | 4 | ... | ... | ... | ... |
| PKS2155−304 | 21:59:08.29 | −30:20:54.2 | 0.0454 | Unkn | 441 | 1.242 | 2 | 0.0453 | 87 | 13.40 | 3 | 0.0453 | <7 | <12.76 | 4 |
| | 21:58:23.81 | −30:19:31.2 | 0.0541 | Early | 567 | 2.235 | 0 | 0.0540 | 315 | 14.06 | 3 | 0.0540 | 32 | 13.63 | 3 |
| | 21:58:40.81 | −30:19:27.1 | 0.0570 | Early | 423 | 1.736 | 0 | 0.0566 | 477 | 14.48 | 3 | 0.0571 | 44 | 13.57 | 3 |

**Notes.**
[a] Spectral type (see the text for the quantitative definition).
[b] Number of additional galaxies within 3 Mpc of the sight line, 400 km s$^{-1}$ of this galaxy, and having $L > 0.1\,L^*$.
**References.** (1) Tripp et al. 2008; (2) Thom & Chen 2008b; (3) Danforth & Shull 2008; (4) Danforth et al. 2006; (5) Penton et al. 2004; (6) Chen & Mulchaey 2009; (9) this paper.

Ly$\alpha$ absorbers to low-$z$ galaxies (Penton et al. 2002; Chen et al. 2005; Chen & Mulchaey 2009; Shone et al. 2010). The much lower cross-correlation amplitudes for systems with $N_{\rm H\,I} < 10^{14}$ cm$^{-2}$ imply that this gas is not physically associated with galaxies. The high amplitude for $N_{\rm H\,I} > 10^{14.5}$ cm$^{-2}$ absorbers, meanwhile, implies a physical association with galaxies. These strong absorbers are sufficiently rare that one may associate each of them with a galaxy. Indeed, the results in Figure 4 suggest that many of the strong absorbers arise within the virialized halos of individual galaxies. Such environments may be the only regions of the universe with sufficient overdensity to give rise to H I column densities exceeding $10^{15}$ cm$^{-2}$.

Another statistical approach to addressing these issues is to compare the observed incidence of Ly$\alpha$ absorption against that predicted for gas surrounding galaxies based on our results and simplified assumptions about the virial radii of galaxies (Equation (1)). Specifically, we ask whether galaxy halos occupy enough area to account for most Ly$\alpha$ absorbers to a given equivalent width limit. To this end, consider the incidence per unit pathlength $dX$ of Ly$\alpha$ absorption $\ell_{\rm Ly\alpha}(X)$, where

$$dX = \frac{H_0}{H(z)}(1+z)^2 dz. \quad (4)$$

At $z = 0$, $dX = dz$ and $\ell(X)$ may be evaluated directly from the observed incidence of absorbers per unit redshift,[17] $\ell(z)$. The quantity $\ell(X)$ is defined to remain constant in time if the product of the comoving number density $n_c$ of objects giving rise to the absorption and the physical size $A_p$ of the sources remains constant, i.e.,

$$\ell(X) = \frac{c}{H_0} n_c A_p. \quad (5)$$

This evaluation assumes that 100% of the area $A_p$ produces detectable absorption. One could include a factor in the formalism that allows for a non-unity covering fraction. Alternatively, one may consider $A_p$ to be the effective area of the object to absorption.

In Figure 8, hatched, colored bands show current estimates for $\ell_{\rm Ly\alpha}(X)$ using results from $z = 0$ surveys of Ly$\alpha$ absorbers (Penton et al. 2004; Wakker & Savage 2009). Each band corresponds to a limiting equivalent width, which for low $W^{\rm Ly\alpha}$ values translates directly to a limiting column density.[18] Overplotted in Figure 8 is a black, solid curve that shows the cumulative inferred contribution to $\ell_{\rm Ly\alpha}(X)$ of virialized galactic halos as a function of galaxy luminosity. For this calculation, we have estimated $n_c$ from the galaxy luminosity function of Blanton et al. (2003) taking $h = 0.72$. We have also assumed that $A_p^{\rm Ly\alpha} = \pi r_{\rm vir}^2$ with $r_{\rm vir}$ given by Equation (1). It is obvious that bright galaxies ($L > L^*$) can only contribute a small fraction of the total incidence of Ly$\alpha$ absorbers. Integrating down to $L = 0.01\,L^*$, the approximate limit of the LCO/WFCCD survey, we infer $\ell_{\rm Ly\alpha}^{r_{\rm vir}}(X; L > 0.01L^*) \approx 15$. Tumlinson & Fang (2005) recovered a similar estimate for galactic halos (in the context of O VI absorption) in an analysis that also accounted for the clustering of galaxies. The estimate lies below all of the $\ell_{\rm Ly\alpha}(X)$ estimates shown in Figure 8, except the strongest Ly$\alpha$ lines ($W^{\rm Ly\alpha} > 300$ mÅ). We conclude, therefore, that *the virialized halos of individual galaxies can only account for the strongest Ly$\alpha$ absorbers ($W^{\rm Ly\alpha} > 300$ mÅ) observed in the low-$z$ IGM*. On the other hand, the results presented in Figures 1–3 indicate systems with $\rho < r_{\rm vir}$ to $L > 0.1\,L^*$ galaxies do exhibit a high covering fraction to $W^{\rm Ly\alpha} > 300$ mÅ absorption. One further concludes that *the majority of strong Ly$\alpha$ absorbers must arise from gas in galactic halos*.

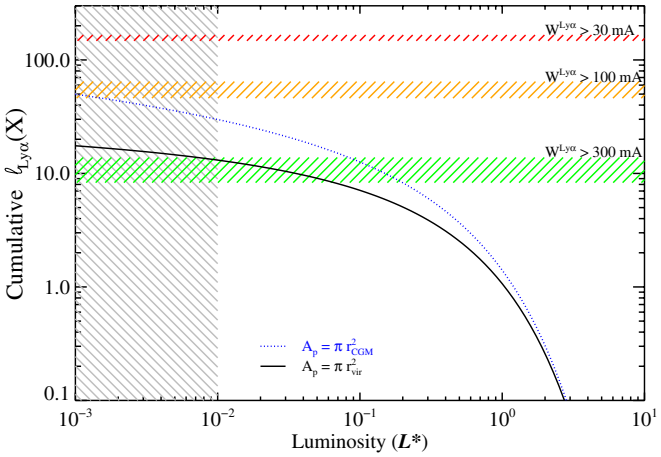


**Figure 8.** Horizontal, hatched regions show measurements for the incidence of Ly$\alpha$ at $z = 0$ as a function of limiting equivalent width (Penton et al. 2004). For strong absorbers ($W^{\rm Ly\alpha} > 300$ mÅ), we observe $\approx$10 lines per unit pathlength (and redshift). The curves represent estimates for $\ell_{\rm Ly\alpha}(X)$ derived from the virialized halos of galaxies (black, solid) and the extended CGM surrounding galaxies (blue, dotted) integrated from a limiting luminosity. The results indicate that the virialized halos of galaxies account only for the incidence of strong Ly$\alpha$ lines observed in the low-$z$ IGM. Even allowing for the extended CGM around each galaxy (with $r_{\rm CGM} = 300$ kpc), the majority of Ly$\alpha$ absorption in the low-$z$ IGM cannot arise from gas surrounding galaxies.

(A color version of this figure is available in the online journal.)

As emphasized throughout this section, galaxies are also surrounded by a CGM with nearly unit covering fraction for $W^{\rm Ly\alpha} > 50$ mÅ to $\rho = 300$ kpc (Figure 6(b)). The dashed blue curve in Figure 8 shows an estimate of the cumulative incidence of Ly$\alpha$ absorbers derived under the assumption that a CGM with $r_{\rm CGM} = 300$ kpc surrounds every galaxy with unit covering fraction, i.e., $A_p^{\rm Ly\alpha} = \pi r_{\rm CGM}^2$, independent of galaxy luminosity. This increases the estimated $\ell_{\rm Ly\alpha}(X)$ value relative to the estimate for virialized halos, especially for galaxies with $r_{\rm vir} \ll 300$ kpc. Nevertheless, even the gas from the extended CGM of galaxies cannot match the observed incidence of weak Ly$\alpha$ absorbers.[19] We conclude that *the overwhelming majority of Ly$\alpha$ lines detected from the IGM arise in structures located at distances beyond several hundred kpc from $L > 0.01\,L^*$ galaxies*. One must seek an additional origin for the majority of IGM absorption than gas surrounding galaxies.

For nearly two decades, researchers have performed hydrodynamic cosmological simulations of the IGM to simulate and study the Ly$\alpha$ forest (e.g., Miralda-Escudé et al. 1996; Gnedin & Hui 1998). This includes several analyses of the low-$z$ IGM (Davé et al. 1999; Cen & Ostriker 1999; Richter et al. 2006; Paschos et al. 2009). Regarding Ly$\alpha$ absorption, the low-$z$ studies have focused primarily on the distributions of H I column density and Doppler parameter and on associating the gas to various phases of the universe. In their recent publication, Davé et al. (2010) have reported that the majority of observable Ly$\alpha$

[17] Commonly referred to as $n(z)$ or $dN/dz$. Similarly $\ell(X)$ is often denoted $dN/dX$.

[18] $W^{\rm Ly\alpha} = 50$ mÅ roughly corresponds to $N_{\rm H\,I} = 10^{13}$ cm$^{-2}$.

[19] Our estimate could be increased by a modest factor if we allowed that one galaxy may give rise to multiple Ly$\alpha$ absorbers. On the other hand, Bowen et al. (2002) have noted that Ly$\alpha$ "clusters" are likely associated with galaxy groups (i.e., multiple galaxies).

absorption (systems with $N_{\rm H\,I} \approx 10^{13}$–$10^{15}$ cm$^{-2}$) is associated with diffuse, photoionized gas at temperatures of $\sim 10^4$ K, with density $n_{\rm H} \approx 10^{-4}$ to $10^{-6}$ cm$^{-3}$, and arising in structures with characteristic sizes of several hundred kpc to 1 Mpc. These structures, which trace large-scale overdensities in the low-$z$ universe, presumably also contain galaxies. In their first paper, Davé et al. (1999) examined the association of galaxies with the IGM and found that the cosmological simulations reasonably reproduced the observed high incidence of Ly$\alpha$ absorption at small impact parameters to galaxies. They also roughly reproduced the observed relation between equivalent width and impact parameter to $\rho \approx 1$ Mpc. The majority of these Ly$\alpha$ absorbers arise in shocked or diffuse gas surrounding the galaxies and the gas is not bound to them. The overall incidence of Ly$\alpha$, meanwhile, is dominated by gas at $\rho \gg 100$ kpc from galaxies. Their results appear, at least qualitatively, to provide a reasonable match to our new observations although we encourage future, quantitative comparison. We are further compelled, therefore, to support this model over ones where virialized halos or the extended CGM associated with discrete galaxies dominate the observed IGM.

The cosmological simulations described above predict that the gas arises in a filamentary network of overdensities, known as the "cosmic web," that permeates the universe. In this same framework, galaxies form within the filaments and galaxy clusters are produced at the nodes where filaments intersect. The observed distribution of galaxies in wide-field surveys generally support this picture (Gott et al. 2009; Bond et al. 2010). Inspired by this paradigm, we introduce a simple filament model to interpret the trends observed in Figure 6. The model assumes that each galaxy in the LCO/WFCCD survey resides at the center of a filamentary structure, generally not at a node. The filaments have a finite width $w$ but are presumed to be infinitely long.[20] In this simple scenario, the covering fraction to Ly$\alpha$ absorption associated with a galaxy is purely geometrical. It is unity for $\rho < w/2$ and decreases at larger values. Overplotted in Figure 6(b) is the predicted covering fraction for this simple model with $w = 400$ kpc. This model shows good agreement with the observations despite its simplicity. It suggests that the overdense structures hosting $z \sim 0$ galaxies have characteristic dimension of several hundred kpc. Indeed, Davé et al. (2010) estimate that $w \sim 400$ kpc corresponds to absorbers with $N_{\rm H\,I} \approx 10^{13.3}$ cm$^{-2}$, a characteristic value for the gas analyzed here. Lastly, if such filaments dominate the incidence of Ly$\alpha$ in the observed IGM then their filling factor of galaxies must be low so that galaxies are only rarely associated with Ly$\alpha$ absorption (Figures 4 and 8). We infer that only rare "patches" of filaments contain $L > 0.01\,L^*$ galaxies.

### 4.2. O VI

Let us now consider O VI gas and its relation to galaxies in the $z \sim 0$ universe. Aside from the H I Lyman series, the most commonly detected absorption lines of the low-$z$ IGM are the O VI doublet. This reflects the high number abundance of oxygen, the ease of identifying a line doublet, and the predominance of regions within the IGM that can produce the $O^{+5}$ ion. With the launch of *HST* and its suite of UV spectrometers, O VI has been surveyed from $z \approx 0.2$–1 (Burles & Tytler 1996; Tripp et al. 2000, 2008; Thom & Chen 2008b; Danforth & Shull 2008). Second, the *FUSE* spectrometer, which operated at $\lambda \approx 910$–1150 Å for nearly a decade, enabled the search for intergalactic O VI down to $z = 0$ (Prochaska et al. 2004; Danforth et al. 2006; Wakker & Savage 2009). Together, these surveys have discovered over 100 O VI doublets to establish their incidence as a function of equivalent width (and column density), to characterize their relation to H I gas, and to measure their distribution of line widths.

Previous work has proposed a variety of origins for this O VI absorption. On the smallest scales, the high incidence of O VI detections in the halo of our Galaxy (Sembach et al. 2003) implies a high filling factor of such gas in the dark matter halos of $L \approx L^*$ galaxies. This assertion has now been confirmed, at least for blue and star-forming $L^*$ galaxies at $z \sim 0.2$ (Tumlinson et al. 2011). At the largest scales (i.e., intergalactic), cosmological simulations predict that the WHIM comprises $\gtrsim$25% of the baryons in the modern universe, and some models also predict that this gas gives rise to a significant fraction of the observed O VI absorption (e.g., Cen & Fang 2006). In between these extremes, the intragroup medium (revealed in some cases by X-ray emission) may have the density and temperature required to yield significant O VI absorption (Mulchaey et al. 1996). Of course, each of these environments is likely to contribute, and each could even dominate at different O VI equivalent width.

A key approach to discriminating among these scenarios is to explore the association between O VI gas and galaxies. Tumlinson & Fang (2005) compared the incidence of O VI absorption against predictions for low-$z$ galaxies as characterized by SDSS and concluded that bright galaxies ($L > L^*$) could not reproduce the observed rate. They suggested that fainter galaxies may explain the observed incidence if dwarf galaxies were surrounded by an enriched medium to ≈200 kpc. Stocke et al. (2006) have correlated $L > 0.1\,L^*$ galaxies with nine O VI absorbers in several fields and reported a median offset of $\approx 180\ h_{70}^{-1}$ kpc. They argued that O VI gas is predominantly associated with individual galaxies and speculated that galaxies with $L < 0.1\,L^*$ dominate. Wakker & Savage (2009) surveyed six field galaxies at $z \approx 0$ with $L \geqslant 0.1\,L^*$ and $\rho < 350$ kpc and reported O VI detections for 2/3. They also argued that gas in the extended surroundings of galaxies contributes significantly to O VI (and Ly$\alpha$) absorption.

The results presented in this paper offer new insight into the origin of O VI at modest to large equivalent widths ($W^{1031} \gtrsim 30$ mÅ). Our survey and analysis have focused on the properties of galaxy halos and the extended CGM as related to Ly$\alpha$ and O VI absorption. In contrast to Ly$\alpha$ (as discussed in the previous subsection), the association between galaxies and O VI shows a strong dependence on galaxy luminosity. In Section 3.1 (Figure 1), we showed that sight lines at impact parameters $\rho < 300$ kpc to dwarf galaxies ($L < 0.1\,L^*$) rarely exhibit O VI absorption. Furthermore, the few dwarfs with associated O VI gas also had a neighboring $L > 0.1\,L^*$ galaxy within $\rho = 200$ kpc of the sight line. The implication is that the extended CGM of dwarf galaxies[21] does not contribute significantly to O VI absorption with $W^{1031} \gtrsim 50$ mÅ. For the brightest galaxies ($L > L^*$), we found a high incidence of O VI detections for $\rho < 225$ kpc but not a single detection beyond (to sensitive limits; Figure 2, Table 4). In Figure 7(b), we have extended the search for O VI associations with $L^*$ galaxies to 1 Mpc. Although there are a few detections for $\rho > 300$ kpc, the majority of these

[20] These filaments also have a finite depth whose dimension is irrelevant to the analysis.

[21] Gas within the virialized halos of dwarf galaxies (i.e., at $\rho \lesssim 50$ kpc), however, was not well probed by our survey.

cases also show an additional, fainter ($L < L^*$) galaxy located within $\rho = 300$ kpc of the sight line. We conclude that the covering fraction of O VI gas around $L^*$ galaxies is small for $\rho \gtrsim 250$ kpc (see also Wakker & Savage 2009).

In contrast to the faint and bright galaxies, the intermediate sub-$L^*$ population exhibits a high incidence of O VI at all impact parameters $\rho < 300$ kpc (Figure 3). This conclusion is independent of spectral type; we find associated O VI for sub-$L^*$ galaxies with early-type (presumed "red and dead") and late-type (star-forming) spectra. Combining these results, we associate O VI gas preferentially with the halos and CGM of sub-$L^*$ galaxies. But this begs the obvious question: are these galaxies sufficiently common that they trace the majority of O VI in the universe? Or does O VI also arise from an additional reservoir, as we found for weak Ly$\alpha$ absorbers?

In Figure 9, we plot the incidence per unit pathlength $dX$ of O VI absorption, $\ell_{\rm O\,VI}(X)$, estimated from the incidence per unit redshift $\ell_{\rm O\,VI}(z)$ measurements of Tripp et al. (2008) for several equivalent width limits. Formally, we have converted their estimates of the incidence per unit redshift $\ell(z)$ measured at $z \approx 0.2$ to $\ell(X)$ (Equation (4)), which implies a downward correction of ≈30%. The widths of the hatched regions indicate the $1\sigma$ uncertainties reported by Tripp et al. (2008) and we caution that systematic bias may have led to a modest overestimate in these $\ell_{\rm O\,VI}(X)$ evaluations (Thom & Chen 2008a). Overlaid on the observational estimates of $\ell_{\rm O\,VI}(X)$, we plot the predicted incidences of O VI from each of our galaxy subsets. The solid bars show the estimated contribution from gas within the virialized halos of each galaxy sample. In each case, we have estimated $n_c$ from the galaxy luminosity function[22] of Blanton et al. (2003) taking $h = 0.72$. For the effective cross-section of halos, we have assumed $A_p^{\rm O\,VI} = \pi r_{\rm vir}^2$ with $r_{\rm vir} = 100, 160$, and 250 kpc for the dwarf, sub-$L^*$, and $L^*$ populations, respectively. These values are somewhat smaller than the value one would derive by averaging Equation (1) over the luminosity function as our estimates for $A_p^{\rm O\,VI}$ include a modest correction for the covering fractions to O VI absorption.

None of the galaxy populations (on their own) can account for the incidence of the commonly observed O VI absorbers if one restricts to virialized halos. For the $L^*$ galaxies, the estimated incidence is ≈10% of the total, in line with the model predictions by Tumlinson & Fang (2005). Furthermore, dwarf galaxies may give rise to as much as 20%–30% of the total incidence but we caution that the estimate shown in Figure 9 assumes a higher covering fraction to O VI for dwarfs than supported by our observations (Figure 1). Together, galactic halos can account for the incidence of very strong O VI absorption ($W^{1031} > 100$ mÅ) and possibly moderate O VI absorbers ($W^{1031} \approx 70$ mÅ). We conclude, however, that *gas in the virialized halos of $z \sim 0$ galaxies with $L > 0.01\,L^*$ cannot account for the majority of observed O VI systems* ($W^{1031} > 30$ mÅ). A similar inference was drawn by Tumlinson & Fang (2005).

The above conclusion is also supported by the results presented in Figure 5, where we found that very few O VI absorbers are coincident with the virialized halo of a galaxy. We further emphasize that the $z \sim 0$ luminosity function is too shallow ($\Phi \propto L^{-1}$) for fainter galaxies to qualitatively modify this conclusion.[23] On the other hand, one may attribute the strongest

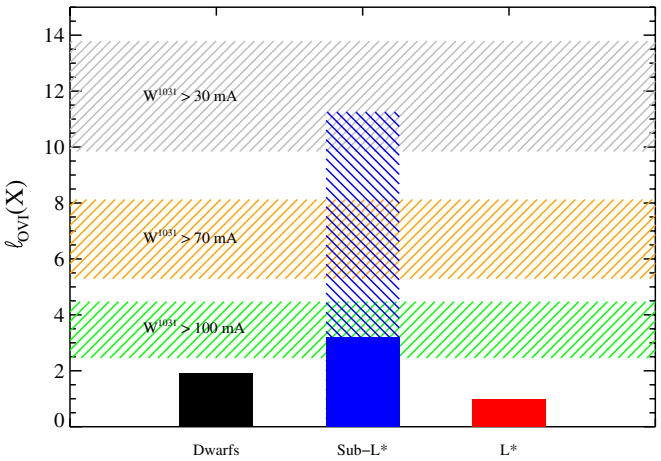


**Figure 9.** Horizontal bands show the observed incidence of O VI absorption per absorption length $\ell_{\rm O\,VI}(X)$, as a function of limiting equivalent width (Tripp et al. 2008). The solid vertical bars indicate estimates of the incidence of O VI absorption for gas in the virialized halos of dwarf (black; $0.01\,L^* < L < 0.1\,L^*$), sub-$L^*$ (blue; $0.1\,L^* < L < L^*$), and $L > L^*$ (red) galaxies. For these estimates we have assumed virial radii of $r_{\rm vir} = 100, 160$, and 250 kpc, respectively, and that the halos have a covering fraction of 100% to O VI. Under this parameterization, virialized halos of galaxies only account for stronger O VI systems. The hatched, blue bar gives the estimate of $\ell_{\rm O\,VI}(X)$ for gas in the extended CGM of sub-$L^*$ galaxies assuming a 100% covering fraction to $\rho = r_{\rm CGM} = 300$ kpc, as suggested by our LCO/WFCCD survey (Figure 3). The excellent correspondence with the observed $\ell_{\rm O\,VI}(X)$ value for $W^{1031} > 30$ mÅ indicates that the remainder of O VI systems arise in this extended CGM. We conclude that the majority of O VI gas observed in the low-$z$ IGM arises in the diffuse medium surrounding individual galaxies (predominantly $L \approx 0.3\,L^*$), and that it rarely originates in the WHIM predicted by cosmological simulations. (A color version of this figure is available in the online journal.)

O VI absorbers ($W^{1031} > 100$ mÅ) to virialized halos and, by inference, galactic-scale processes. In fact, one must conclude from the results presented in Figures 1–3, 5, and 9 that the majority of strong ($W^{1031} > 100$ mÅ) O VI systems arise from within the halos of individual galaxies. We emphasize that this does not contradict our conclusion from above that relates to weaker O VI systems.

With virialized halos ruled out as the dominant origin of O VI gas (by frequency of absorption, not necessarily by mass), we now consider the extended CGM surrounding $z \sim 0$ galaxies. As emphasized above, we find a significant covering fraction to $\rho = 300$ kpc for the sub-$L^*$ galaxies (Figure 3). Overlaid on the $\ell_{\rm O\,VI}(X)$ estimate for virialized halos of the sub-$L^*$ galaxies is a hatched bar that represents the contribution to $\ell_{\rm O\,VI}(X)$ from an extended CGM surrounding each sub-$L^*$ galaxy. This hatched bar assumes $A_p^{\rm O\,VI} = \pi r_{\rm CGM}^2$ with $r_{\rm CGM} = 300$ kpc and a 100% covering fraction for $W^{1031} \geqslant 30$ mÅ. This amounts to a several times higher incidence of O VI absorption. Remarkably, we find that the extended CGM of sub-$L^*$ galaxies reproduces the incidence of all O VI absorbers with $W^{1031} \gtrsim 30$ mÅ. Of course, these results follow from the close association of galaxies with O VI absorbers (Figure 5) and the high covering fraction of O VI gas surrounding sub-$L^*$ galaxies (Figure 3). While one could reduce this estimate by a factor of order unity (e.g., by assuming a smaller covering fraction), *we conclude that the extended CGM of sub-$L^*$ galaxies is the primary reservoir of O VI gas observed in the $z \sim 0$ IGM*. This final conclusion, which draws a distinction between virialized halos of sub-$L^*$ galaxies and their extended CGM, is sensitive to the precise definition of a galaxy halo and its radius. We encourage additional theoretical

[22] For the dwarf galaxy calculation, we limit the integration to $0.01\,L^* < L < 0.1\,L^*$.

[23] Although there remains debate on the precise slope of the faint end, one would require a much steeper slope than currently estimated for faint galaxies to significantly contribute.

exploration into the nature and extent of virialized gas in the halos of subluminous, low-$z$ galaxies.

An additional inference that may be drawn from these results is that the extended CGM is sufficient to explain *all* metal-line absorption observed along quasar sight lines. This follows simply from the fact that O VI is the metal transition of highest observed incidence. We speculate that essentially all metals attributed to the IGM are associated with the halos and CGM of $L > 0.01\,L^*$ galaxies.

Let us now consider the implications of an extended CGM that gives rise to significant O VI absorption surrounding sub-$L^*$ galaxies. First, we note that this CGM may include neighboring galaxies, the intragroup medium, and the diffuse medium that envelops the galaxies (e.g., filaments). Regarding neighboring galaxies,[24] we have already demonstrated that virialized halos contribute only modestly to the incidence of O VI. By the same argument, they cannot dominate the detections associated with the extended CGM of sub-$L^*$ galaxies. Regarding the intragroup medium, only a subset of sub-$L^*$ galaxies exhibit galaxy overdensities suggestive of a group (Table 5). We infer, therefore, that this extended CGM is best described by a diffuse, modestly overdense ($\delta \gtrsim 10$) medium. In the IGM paradigm of undulating Gunn–Peterson absorption, such overdensities naturally give rise to significant H I absorption. Indeed, as discussed above, Ly$\alpha$ absorption is a ubiquitous phenomenon for galaxies of all luminosity, and every intervening O VI absorber[25] detected to date shows corresponding Ly$\alpha$ absorption (Thom & Chen 2008b).

Although one may naturally expect H I absorption from an overdense region of the universe, the detection of O VI further requires a chemically enriched medium and the physical conditions that produce the $O^{+5}$ ion. Regarding the former, our results require that the CGM of sub-$L^*$ has been polluted by metals on scales of several hundred kpc. Although many of the sub-$L^*$ galaxies in our sample show the spectral signatures of ongoing star formation, these are not star-bursting systems, and they are unlikely to currently be driving galactic-scale winds to such large distances. We infer, therefore, that this CGM was previously enriched. Current estimates for the metallicites of the O VI absorbers suggest values ranging from 0.01 to nearly solar abundance with a median of $\approx$0.1 solar (e.g., Prochaska et al. 2004; Cooksey et al. 2008; Thom & Chen 2008a; Danforth & Shull 2008). This enrichment level exceeds predictions from the first stars (e.g., Wise et al. 2010), indicating that a subsequent phase of star formation is required. The medium is too diffuse to form metals in situ and, therefore, these must have been transported by distances of 100 kpc or more. The proximity of the sub-$L^*$ galaxy suggests that the oxygen was produced in that system, yet this is purely speculative. We also note, following the mass estimate from Section 4.1 (Equation (3)), that a 0.1 solar metallicity implies a metal mass equivalent to $\approx 3 \times 10^9 M_\odot$ of solar metallicity stars. This could exceed the total mass in metals within a typical sub-$L^*$ galaxy and its satellites, which would require mass outflow rates from galactic winds that match or exceed the star formation rate (e.g., Weiner et al. 2009). Comprehensive modeling of the chemical enrichment of the IGM that includes galaxy formation and metal transport are required to further explore this topic (e.g., Cen & Ostriker 2006; Ganguly et al. 2008; Oppenheimer & Davé 2008, 2009).

In addition to containing oxygen, this CGM must have the appropriate density and/or temperature for a significant fraction of oxygen to exist as $O^{+5}$. One process to produce $O^{+5}$ is via collisional ionization (CI) which requires temperatures on the order of $T \sim 10^5$–$10^6$ K. The other obvious mechanism to produce $O^{+5}$ is with photoionization, which requires photons with energies $h\nu > 8$ Ryd. Such hard photons are only produced by AGNs, and the extragalactic UV background (EUVB) is the obvious source of such radiation when one is far from active galaxies.

Consider first several inferences one may draw from our association of O VI with the extended CGM of sub-$L^*$ galaxies. If the extended CGM (almost by definition) lies beyond the virialized radius of these galaxies, one may not expect a collisionally ionized medium. Furthermore, the majority of these sub-$L^*$ galaxies are not obviously located within a larger dark matter halo (e.g., a group or cluster). Therefore, this gas may not have been virialized to $T \gg 10^4$ K. One would require instead gravitationally induced shock heating from larger scales. Indeed, the collapse of large-scale density "waves" is predicted to drive the production of the WHIM in cosmological simulations (e.g., Cen & Ostriker 1999; Davé et al. 2001) and may, in principle, heat the CGM of sub-$L^*$ galaxies. Although this is plausible, these waves are generally predicted to "crash" on larger scales (many Mpc) than the several hundred kpc scales of the CGM. Indeed, Ganguly et al. (2008) analyzed the average impact parameter to galaxies of O VI gas arising in the WHIM. They found in their simulations that only $\approx$1% of O VI detections with $W^{1031} \geqslant 50$ mÅ would have a $L > 0.01\,L^*$ galaxy within 300 kpc. This prediction is strongly ruled out by our observations (see also Wakker & Savage 2009). By inference, we conclude that *O VI gas observed in the low-z IGM does not typically trace a collisionally ionized WHIM*.

Empirically, the ionization mechanism for observed O VI absorbers remains a matter of great debate. We support (and have contributed to) arguments that conclude most O VI systems are not collisionally ionized (Prochaska et al. 2004; Tripp et al. 2008; Thom & Chen 2008a; Howk et al. 2009). The evidence includes the close alignment of H I gas with O VI, the narrowness of the coincident Ly$\alpha$ absorption (and of O VI itself), and the very frequent detection of coincident C III absorption. On the other hand, see Fox (2011) for a set of arguments against O VI arising in predominantly photoionized gas. Given the results presented above, we may at least consider whether a photoionized, extended CGM of sub-$L^*$ galaxies may naturally support O VI absorption.

Under the assumptions that the gas is optically thin to ionizing radiation and that the UV radiation field is dominated by a typical AGN spectrum ($f_\nu \propto \nu^{-1.6}$), standard photoionization calculations indicate that an ionization parameter[26] $U \gtrsim 10^{-1}$ is required to produce a significant fraction of $O^{+5}$ ions. To achieve $U \gtrsim 10^{-1}$ with current estimates for the EUVB (e.g., CUBA (Cosmic Ultraviolet Background), which predicts $J_\nu \approx 10^{-25}$ erg s$^{-1}$ Hz$^{-1}$ cm$^{-2}$ at 8 Ryd; Haardt & Madau 1996), this demands a volume density $n_{\rm H} \lesssim 10^{-5}$ cm$^{-3}$. This value is roughly 50$\times$ the mean baryonic density at $z \sim 0$ suggesting an overdensity $\delta \lesssim 50$. These same photoionization calculations imply a size for the structure of $d \sim 300$ kpc $(N_{\rm H\,I}/10^{14}\,{\rm cm}^{-2})$. The constraints on $n_{\rm H}$ and $d$ give plausible values for the extended CGM of sub-$L^*$ galaxies. They imply a gas that is overdense yet not virialized ($\delta \ll 200$). Furthermore,

[24] Also, by definition the volume beyond $r_{\rm vir}$ must have a lower density than the medium within it.

[25] Tripp et al. (2008) report a set of O VI systems within 3000 km s$^{-1}$ of the quasar that has no coincident Ly$\alpha$ absorption.

[26] $U \equiv \Phi/cn_{\rm H}$, where $\Phi$ is the flux of ionizing photons.

the inferred size of the structures coincides with the dimensions inferred from our analysis. We conclude that the gas in the extended CGM could be predominantly photoionized material giving rise to O VI absorption.

We have developed the following picture for O VI absorption in the low-$z$ IGM: the gas has density $n_{\rm H} \approx 10^{-5}\,{\rm cm}^{-3}$, is predominantly photoionized, and is primarily located in the extended CGM of sub-$L^*$ galaxies. The oxygen was produced in a previous episode of star formation (perhaps by the observed sub-$L^*$ galaxy) and has been transported to the CGM by one or more processes. Remarkably, this scenario is qualitatively consistent with the model for O VI described by Oppenheimer & Davé (2009; see also Tepper-García et al. 2011; Smith et al. 2011). In their cosmological simulations, oxygen is produced at earlier times (often $z > 1$) in a star-bursting galaxy whose galactic-scale wind transports the metals to the surrounding, overdense IGM. This gas is observed today primarily as photoionized O VI and is coupled to significant H I absorption mainly because both exist in overdense regions.

Oppenheimer & Davé (2009) studied the equivalent width and Doppler parameter distribution of O VI gas and found that their model gives reasonably good agreement to the observed distribution.[27] These authors also performed a qualitative analysis on the connection between O VI absorption and galaxies (their Figures 14 and 15). They found O VI gas is generally located at several virial radii (∼100–300 kpc) from galaxies with masses $M_{\rm gal} \sim 10^{9.5}$–$10^{10}\,M_\odot$ (∼0.03–0.1 $M^*$). Although these separations are consistent with our results, the typical galaxy mass may be lower than that of the average sub-$L^*$ galaxy. We encourage further analysis to consider the covering fraction to O VI absorption as a function of galaxy luminosity (e.g., Ganguly et al. 2008). The data also permit one to examine trends between the galactic mass and environment with the observed equivalent widths of absorption.

Before concluding, it is worth speculating on why the extended CGM for $L^*$ and dwarf galaxies would have a lower covering fraction than that observed for sub-$L^*$ galaxies. Regarding dwarf galaxies, there are several plausible explanations. First, these galaxies generally show lower $N_{\rm H\,I}$ values on average suggesting lower total gas columns. Second, it is possible that the CGM of dwarf galaxies is chemically poor in comparison to brighter galaxies.[28] Lastly, the physical conditions of the gas (temperature, density) in the CGM surrounding dwarf galaxies may not support the $O^{+5}$ ion, e.g., the gas may have too low a volume density. Together, these effects could reduce the associated O VI absorption to equivalent widths below typical detection limits.

For the $L^*$ galaxies, however, we observe H I column densities at least as large as those observed for the sub-$L^*$ galaxies (Table 6). One may also expect the gas to have higher metallicity.[29] If the lower incidence of O VI absorption is unrelated to differences in chemical enrichment, then the result must relate to the physical conditions of the gas, i.e., the extended CGM of $L^*$ galaxies has a density and/or temperature that is not favorable for $O^{+5}$ ions. Under the assumption of photoionization by the EUVB, the gas must have $n_{\rm H} \approx 10^{-5}\,{\rm cm}^{-3}$ for its ionization potential to favor $O^{+5}$ ions. If the CGM of $L^*$ galaxies is ≈10× higher than that of sub-$L^*$ galaxies at $\rho \sim 200$ kpc, then this could explain the preponderance of non-detections. In this scenario, one would predict the detection of metals at $\rho \sim 200$ kpc from $L^*$ galaxies in lower ionization states (e.g., C IV, C III). One might then expect a higher incidence of detections at somewhat larger impact parameters,[30] but this is not observed (Figure 7(b)). As another alternative, it is possible that gas at $\rho \sim 250$ kpc from an $L^*$ galaxy has been shock heated to $T \gg 10^5$ K. Indeed, these galaxies are more frequently members of a group, i.e., embedded within a larger, virialized halo. Lastly, the modes in which galaxies accrete their gas could also influence the detection of O VI absorption (e.g., via cold streams or cooling clumps from a hot phase; Maller & Bullock 2004; Kereš & Hernquist 2009).

## 5. SUMMARY

With this paper we have examined the associations of galaxies with Ly$\alpha$ and O VI absorption in the low-$z$ IGM to explore the origin of this gas. Specifically, we have correlated galaxies from our LCO/WFCCD galaxy survey (Prochaska et al. 2011) and IGM absorption from published line lists of *HST* and *FUSE* UV quasar spectra. These two data sets are essentially independent of one another, although we have supplemented the IGM line lists with our own analysis of the quasar sight lines. Our main findings are summarized as follows.

1. Galaxies of all luminosity ($L > 0.01\,L^*$) and spectral type show strong, associated Ly$\alpha$ absorption to impact parameter $\rho \approx 300$ kpc with a very high covering fraction (≈90%). The strongest H I absorbers ($W^{\rm Ly\alpha} \gtrsim 1$ Å) are preferentially associated with brighter galaxies ($L > 0.1\,L^*$).
2. We estimate a baryonic mass for this extended CGM of $M_{\rm CGM} \approx 3 \times 10^{10} M_\odot\ (N_{\rm H,CGM}/10^{19}\,{\rm cm}^{-2})(r_{\rm CGM}/300\,{\rm kpc})^2$, having adopted a constant H I column density $N_{\rm H,CGM}$.
3. Galaxies with luminosities $L > 0.1\,L^*$ exhibit a high covering fraction (>80%) for significant O VI absorption to $\rho = 200$ kpc and to 300 kpc for sub-$L^*$ galaxies. Dwarf galaxies ($L < 0.1\,L^*$) exhibit a low covering fraction for $\rho > 50$ kpc.
4. Despite these high covering fractions of Ly$\alpha$ and O VI absorption, there are examples of non-detections to very sensitive limits, even at very low impact parameters ($\rho \lesssim 50$ kpc).
5. We observe a declining covering fraction and median equivalent width for Ly$\alpha$ to $\rho = 1$ Mpc. The equivalent widths of the positive detections at $\rho > 100$ kpc may be described by a power law, $W^{\rm Ly\alpha}(\rho) = 3.3\,{\rm Å}\,(\rho/1\,{\rm kpc})^{-0.43}$, but with great scatter.
6. To $\rho = 1$ Mpc, $L^*$ galaxies show two distinct distributions of Ly$\alpha$ absorption: (1) a set of positive detections with $W^{\rm Ly\alpha} > 200$ mÅ and (2) a set of non-detections with $W^{\rm Ly\alpha} < 50$ mÅ.
7. The detection rate of Ly$\alpha$ absorption with impact parameter may be described by galaxies within filaments having characteristic widths $w \sim 400$ kpc.

[27] These authors had to include turbulent broadening, added in post-processing, to explain the observed linewidths of O VI (supported in part by Tripp et al. 2008).

[28] An ongoing Cycle 18 *HST*/COS program will assess the chemical enrichment of gas associated with dwarf galaxies (PI: Tumlinson; 1224).

[29] Although, one could also speculate that the larger potential well of $L^*$ galaxies prevents the transport of metals beyond their virialized halos (e.g., Oppenheimer & Davé 2008). This hypothesis, however, is apparently not supported by current research on galactic-scale winds (e.g., Weiner et al. 2009; Rubin et al. 2010).

[30] Also, low column densities at all impact parameters if one assumes spherical symmetry.

8. Few, if any, of the weak Ly$\alpha$ absorbers ($W^{\rm Ly\alpha} < 100$ mÅ) from the low-$z$ IGM arise in the virialized halos of $z \sim 0$ galaxies or their surrounding CGM. The majority of strong Ly$\alpha$ absorbers ($W^{\rm Ly\alpha} > 300$ mÅ), however, does arise in these environments.
9. The strongest O VI absorbers ($W^{1031} > 100$ mÅ; $N_{\rm O\,VI} > 10^{14}$ cm$^{-2}$) arise preferentially in the galactic halos of $L > 0.01\,L^*$ galaxies. Weaker O VI absorbers are associated with the extended CGM of sub-$L^*$ galaxies.
10. Current predictions for models where O VI gas arises in a collisionally ionized WHIM are ruled out at high confidence. We suggest that O VI gas is primarily associated with a photoionized CGM with $n_{\rm H} \approx 10^{-5}$ cm$^{-3}$ and typical dimension $d \sim 300$ kpc.

J.X.P. is partially supported by an NSF CAREER grant (AST 0548180). We acknowledge valuable comments and criticism of this work from B. Oppenheimer, G. Worseck, J. Tumlinson, and A. Fox. We acknowledge valuable assistance from R. da Silva.

## REFERENCES


Bahcall, J. N., & Spitzer, L. J. 1969, ApJ, 156, L63
Barton, E. J., & Cooke, J. 2009, AJ, 138, 1817
Bergeron, J. 1986, A&A, 155, L8
Bergeron, J., & Boisse, P. 1991, Adv. Space Res., 11, 241
Blanton, M. R., Hogg, D. W., Bahcall, N. A., et al. 2003, ApJ, 594, 186
Bond, N. A., Strauss, M. A., & Cen, R. 2010, MNRAS, 409, 156
Bowen, D. V., & Chelouche, D. 2011, ApJ, 727, 47
Bowen, D. V., Jenkins, E. B., Tripp, T. M., et al. 2008, ApJS, 176, 59
Bowen, D. V., Pettini, M., & Blades, J. C. 2002, ApJ, 580, 169
Bregman, J. N., Miller, E. D., Athey, A. E., & Irwin, J. A. 2005, ApJ, 635, 1031
Burles, S., & Tytler, D. 1996, ApJ, 460, 584
Cen, R., & Fang, T. 2006, ApJ, 650, 573
Cen, R., & Ostriker, J. P. 1999, ApJ, 514, 1
Cen, R., & Ostriker, J. P. 2006, ApJ, 650, 560
Chen, H., Helsby, J. E., Gauthier, J., et al. 2010, ApJ, 714, 1521
Chen, H., Lanzetta, K. M., Webb, J. K., & Barcons, X. 1998, ApJ, 498, 77
Chen, H., & Mulchaey, J. S. 2009, ApJ, 701, 1219
Chen, H.-W., Lanzetta, K. M., & Webb, J. K. 2001a, ApJ, 556, 158
Chen, H.-W., Lanzetta, K. M., Webb, J. K., & Barcons, X. 2001b, ApJ, 559, 654
Chen, H.-W., & Prochaska, J. X. 2000, ApJ, 543, L9
Chen, H.-W., Prochaska, J. X., Weiner, B. J., Mulchaey, J. S., & Williger, G. M. 2005, ApJ, 629, L25
Chen, H.-W., & Tinker, J. L. 2008, ApJ, 687, 745
Cooksey, K. L., Prochaska, J. X., Chen, H.-W., Mulchaey, J. S., & Weiner, B. J. 2008, ApJ, 676, 262
Cooksey, K. L., Thom, C., Prochaska, J. X., & Chen, H. 2010, ApJ, 708, 868
Courteau, S., Dutton, A. A., van den Bosch, F. C., et al. 2007, ApJ, 671, 203
Danforth, C. W., & Shull, J. M. 2008, ApJ, 679, 194
Danforth, C. W., Shull, J. M., Rosenberg, J. L., & Stocke, J. T. 2006, ApJ, 640, 716
Davé, R., Cen, R., Ostriker, J. P., et al. 2001, ApJ, 552, 473
Davé, R., Hernquist, L., Katz, N., & Weinberg, D. H. 1999, ApJ, 511, 521
Davé, R., Oppenheimer, B. D., Katz, N., Kollmeier, J. A., & Weinberg, D. H. 2010, MNRAS, 408, 2051
Dunkley, J., Komatsu, E., Nolta, M. R., et al. 2009, ApJS, 180, 306
Fox, A. J. 2011, ApJ, 730, 58
Freeland, E., Cardoso, R. F., & Wilcots, E. 2008, ApJ, 685, 858
Ganguly, R., Cen, R., Fang, T., & Sembach, K. 2008, ApJ, 678, L89
Gauthier, J.-R., Chen, H.-W., & Tinker, J. L. 2010, ApJ, 716, 1263
Gnedin, N. Y., & Hui, L. 1998, MNRAS, 296, 44
Gott, J. R., Choi, Y., Park, C., & Kim, J. 2009, ApJ, 695, L45
Haardt, F., & Madau, P. 1996, ApJ, 461, 20
Hibbard, J. E., van Gorkom, J. H., Rupen, M. P., & Schiminovich, D. 2001, in ASP Conf. Ser. 240, Gas and Galaxy Evolution, ed. J. E. Hibbard, M. Rupen, & J. H. van Gorkom (San Francisco, CA: ASP), 657
Howk, J. C., Ribaudo, J. S., Lehner, N., Prochaska, J. X., & Chen, H. 2009, MNRAS, 396, 1875
Jenkins, E. B., & Meloy, D. A. 1974, ApJ, 193, L121
Kereš, D., & Hernquist, L. 2009, ApJ, 700, L1
Lanzetta, K. M., Bowen, D. V., Tytler, D., & Webb, J. K. 1995, ApJ, 442, 538
Lehner, N., Prochaska, J. X., Kobulnicky, H. A., et al. 2009, ApJ, 694, 734
Lehner, N., Savage, B. D., Richter, P., et al. 2007, ApJ, 658, 680
Maller, A. H., & Bullock, J. S. 2004, MNRAS, 355, 694
McDonald, P., Seljak, U., Burles, S., et al. 2006, ApJS, 163, 80
Miralda-Escudé, J., Cen, R., Ostriker, J. P., & Rauch, M. 1996, ApJ, 471, 582
Mo, H. J., & Miralda-Escude, J. 1996, ApJ, 469, 589
Morris, S. L., & Jannuzi, B. T. 2006, MNRAS, 367, 1261
Morris, S. L., Weymann, R. J., Dressler, A., et al. 1993, ApJ, 419, 524
Mulchaey, J. S., Davis, D. S., Mushotzky, R. F., & Burstein, D. 1996, ApJ, 456, 80
Narayanan, A., Wakker, B. P., & Savage, B. D. 2009, ApJ, 703, 74
Oppenheimer, B. D., & Davé, R. 2008, MNRAS, 387, 577
Oppenheimer, B. D., & Davé, R. 2009, MNRAS, 395, 1875
Oppenheimer, B. D., Davé, R., Katz, N., Kollmeier, J. A., & Weinberg, D. H. 2011, arXiv:1106.1444
Paschos, P., Jena, T., Tytler, D., Kirkman, D., & Norman, M. L. 2009, MNRAS, 399, 1934
Penton, S. V., Stocke, J. T., & Shull, J. M. 2002, ApJ, 565, 720
Penton, S. V., Stocke, J. T., & Shull, J. M. 2004, ApJS, 152, 29
Prochaska, J. X., Chen, H.-W., Howk, J. C., Weiner, B. J., & Mulchaey, J. 2004, ApJ, 617, 718
Prochaska, J. X., & Tumlinson, J. 2009, in Astrophysics in the Next Decade, ed. H. A. Thronson, M. Stiavelli, & A. Tielens (Berlin: Springer), 419
Prochaska, J. X., Weiner, B., Chen, H.-W., Cooksey, K. L., & Mulchaey, J. S. 2011, ApJS, 193, 28
Prochaska, J. X., Weiner, B. J., Chen, H.-W., & Mulchaey, J. S. 2006, ApJ, 643, 680
Rauch, M. 1998, ARA&A, 36, 267
Richter, P., Fang, T., & Bryan, G. L. 2006, A&A, 451, 767
Rubin, K. H. R., Weiner, B. J., Koo, D. C., et al. 2010, ApJ, 719, 1503
Savage, B. D., & de Boer, K. S. 1979, ApJ, 230, L77
Savage, B. D., Lehner, N., Wakker, B. P., Sembach, K. R., & Tripp, T. M. 2005, ApJ, 626, 776
Savage, B. D., & Sembach, K. R. 1991, ApJ, 379, 245
Savage, B. D., Sembach, K. R., Jenkins, E. B., et al. 2000, ApJ, 538, L27
Savage, B. D., Sembach, K. R., Wakker, B. P., et al. 2003, ApJS, 146, 125
Sembach, K. R., Tripp, T. M., Savage, B. D., & Richter, P. 2004, ApJS, 155, 351
Sembach, K. R., Wakker, B. P., Savage, B. D., & Richter, P. 2006, in ASP Conf. Ser. 348, Astrophysics in the Far Ultraviolet: Five Years of Discovery with FUSE, ed. G. Sonneborn, H. W. Moos, & B.-G. Andersson (San Francisco, CA: ASP), 375
Sembach, K. R., Wakker, B. P., Savage, B. D., et al. 2003, ApJS, 146, 165
Shone, A. M., Morris, S. L., Crighton, N., & Wilman, R. J. 2010, MNRAS, 402, 2520
Shull, J. M., Tumlinson, J., & Giroux, M. L. 2003, ApJ, 594, L107
Smith, B. D., Hallman, E. J., Shull, J. M., & O'Shea, B. W. 2011, ApJ, 731, 6
Spinrad, H., Filippenko, A. V., Yee, H. K., et al. 1993, AJ, 106, 1
Spitzer, L., Jr. 1956, ApJ, 124, 20
Stocke, J. T., Penton, S. V., Danforth, C. W., et al. 2006, ApJ, 641, 217
Tepper-García, T., Richter, P., Schaye, J., et al. 2011, MNRAS, 413, 190
Thom, C., & Chen, H. 2008a, ApJS, 179, 37
Thom, C., & Chen, H. 2008b, ApJ, 683, 22
Tripp, T. M., Aracil, B., Bowen, D. V., & Jenkins, E. B. 2006a, ApJ, 643, L77
Tripp, T. M., Aracil, B., Bowen, D. V., & Jenkins, E. B. 2006b, ApJ, 643, L77
Tripp, T. M., Jenkins, E. B., Bowen, D. V., et al. 2005, ApJ, 619, 714
Tripp, T. M., Jenkins, E. B., Williger, G. M., et al. 2002, ApJ, 575, 697
Tripp, T. M., Lu, L., & Savage, B. D. 1998, ApJ, 508, 200
Tripp, T. M., Savage, B. D., & Jenkins, E. B. 2000, ApJ, 534, L1
Tripp, T. M., Sembach, K. R., Bowen, D. V., et al. 2008, ApJS, 177, 39
Tumlinson, J., & Fang, T. 2005, ApJ, 623, L97
Tumlinson, J., Shull, J. M., Giroux, M. L., & Stocke, J. T. 2005, ApJ, 620, 95
Tumlinson, J., et al. 2011, Science, submitted
Viel, M., Bolton, J. S., & Haehnelt, M. G. 2009, MNRAS, 399, L39
Wakker, B. P., & Savage, B. D. 2009, ApJS, 182, 378
Weiner, B. J., Coil, A. L., Prochaska, J. X., et al. 2009, ApJ, 692, 187
Weymann, R. J., Jannuzi, B. T., Lu, L., et al. 1998, ApJ, 506, 1
Williger, G. M., Heap, S. R., Weymann, R. J., et al. 2006, ApJ, 636, 631
Wilman, R. J., Morris, S. L., Jannuzi, B. T., Davé, R., & Shone, A. M. 2007, MNRAS, 375, 735
Wise, J. H., Turk, M. J., Norman, M. L., & Abel, T. 2010, arXiv:1011.2632
York, D. G. 1974, ApJ, 193, L127
Zehavi, I., Zheng, Z., Weinberg, D. H., et al. 2011, ApJ, 736, 59
Zheng, Z., Coil, A. L., & Zehavi, I. 2007, ApJ, 667, 760